

Neutron Irradiation

Experimental Physics

Student Notes

1 AIM

To measure the half-lives of some of the radio-nuclides produced in the thermal neutron irradiation of indium and silver metals, and to study the growth of the induced activity as a function of irradiation time.

2 INTRODUCTION

Neutrons can only be liberated in nuclear reactions e.g. induced or spontaneous nuclear fission, or the reactions of nuclear particles from accelerators or radioactive nuclei with light target nuclei. Because neutrons carry no charge, their interaction with atomic electrons is very small¹ and the main interactions of neutrons with matter occur via nuclear processes such as nuclear reactions or elastic and inelastic scattering of neutrons by nuclei. The absence of a Coulomb barrier means that even very low energy neutrons will enter and react with nuclei. In fact, it is found experimentally that low energy (0.01 eV to 0.1 eV) neutrons have particularly high probabilities of reacting with nuclei. Neutrons produced by the processes mentioned above, however, normally have energies in the MeV range and need to be slowed down before they can be usefully employed.

Fast neutrons may be slowed down or moderated by undergoing a series of elastic collisions with the nuclei in a mass of substance called a moderator. After many successive collisions, the neutron energy is distributed among the moderated atoms and the neutron finishes up with an energy equal to the average energy which an atom in the moderator possesses due to its thermal motion ($kT \approx 0.025$ eV at room temperature). In a good moderator, neutrons should be thermalised in as few collisions as possible and the probability of neutron absorption by the moderator's nuclei should be small.

Neutrons find many uses in industry, medicine and the sciences. Neutron moderation forms the basis of some industrial techniques of moisture gauging (e.g. in soil and cement) and the measurement of hydrocarbon content (e.g. of rocks; as in oil-well logging).

¹In magnetic materials, however, the neutron's magnetic dipole moment can interact with the dipole moments of the magnetic atoms' electrons. This interaction forms the basis of neutron diffraction studies of magnetic material structures.

Neutron irradiation of the elements gives many radio-nuclides useful as tracers in industry and medicine, and neutron activation analysis may be used to detect trace amounts of the elements. In the latter technique, a sample is irradiated with thermal neutrons and from a study of the energy spectra and half-lives of the resulting isotopes the relative amounts of the elements constituting the sample may be determined.

In this experiment (a rudimentary activation analysis?) you will measure the half lives of some nuclides produced in the irradiation of Ag and In and also study some properties of neutron moderators and absorbers.

3 THEORY

Consider a large number n , of identical radioactive nuclei. If the probability of any one nucleus decaying is independent of the other nuclei then the **decay rate** of the nuclei is proportional to the number of nuclei present at a given time t , i.e.

$$-\frac{dn}{dt} = \lambda n \quad (1)$$

where the proportionality constant λ , is known as the decay constant. Integration of equation (1) leads to

$$n = n_0 e^{-\lambda t} \quad (2)$$

where n_0 is the number of nuclei present at time $t = 0$. The half life $\tau_{1/2}$, defined as the time taken for the number of nuclei to decrease to half the original value, is then given by:

$$\tau_{1/2} = \ln 2 / \lambda \quad (3)$$

(Can you show this?)

NOTE: In a typical nuclear counting experiment we do not measure n or dn/dt directly. The observed count rate c , is proportional to the decay rate of the radioactive species i.e.:

$$c = K \left(-\frac{dn}{dt} \right) = k \lambda n \quad \text{where } K \text{ is a constant.} \quad (4)$$

Consider now the situation where a number of target nuclei, n_T , is exposed to a flux ϕ (dimensions: neutrons /area /time) of neutrons. Let σ (dimensions: area /nucleus) be the neutron capture cross-section i.e. the probability per nucleus of neutron capture and transformation of the target nucleus to a nucleus whose mass number is increased by one. If the product nuclei are radioactive and decay with a decay constant λ , then the time rate of change of the number of product nuclei n , is given by:

$$\frac{dn}{dt} = \phi \sigma n T - \lambda n \quad (5)$$

which integrates to give

$$n = \frac{\phi\sigma n_T}{\lambda} (1 - e^{-\lambda t}) \quad (6)$$

It is seen from equation (5) that for long irradiation times ($t \gg 1/\lambda$) $n \rightarrow \phi\sigma n_T/\lambda$, i.e. if n_T is assumed constant, the number of product nuclei **saturates** since eventually the product nuclei decay as fast as they are being formed by the neutrons.

4 APPARATUS

4.1 Irradiation

The neutron source consists of 20 GBq (1 Bq = 1 Becquerel = 1 disintegration/sec) of americium-241 intimately mixed with beryllium powder and sealed in a stainless steel cylinder 22 mm in diameter and 31 mm long. The Am-241 ($\tau_{1/2} = 433$ years) emits α -particles which react with the Be to produce neutrons according to the reaction:



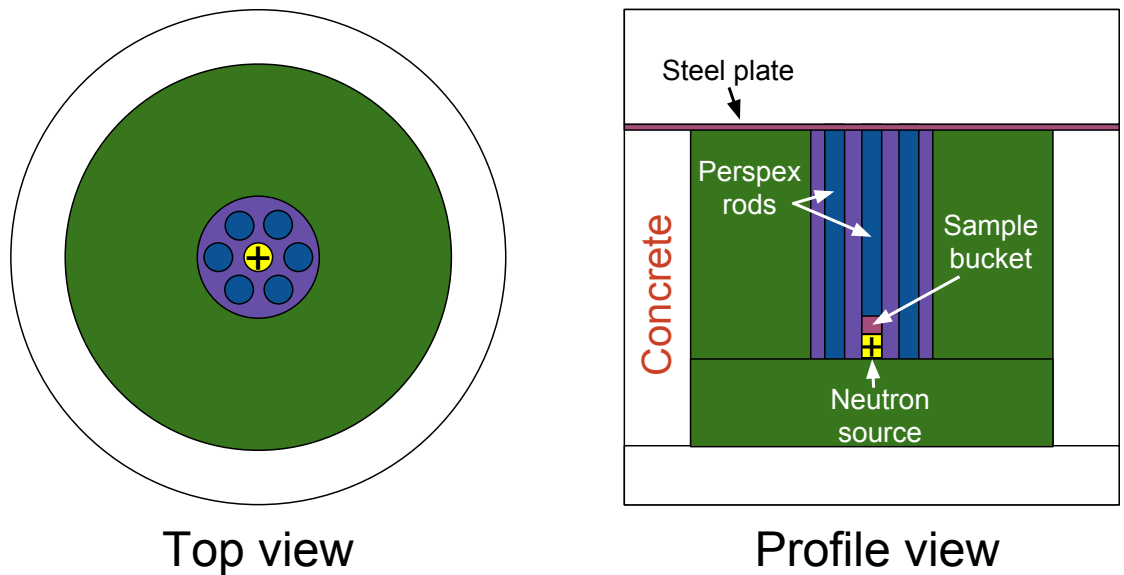
where $Q = 5.7$ MeV is the energy liberated in the reaction due to mass losses. Since the α -particles are emitted with energies ~ 5.5 MeV, the neutrons can have initial energies up to ~ 11 MeV, however, it is found experimentally that the neutron energy spectrum peaks at about 3.5 MeV. About 10^6 neutrons/sec are emitted by the source used in this experiment.

To slow the neutrons to thermal energies, the source is situated in a well in the centre of a cylindrical paraffin moderating block encased in concrete. Four other wells, symmetrically spaced around the central well, are used for specimen irradiation. The specimens are separated from the source by about 40 mm of paraffin, this being a compromise between the greater thickness (~ 200 mm) necessary to completely thermalize the neutrons and the smaller distance needed due to the reduction of neutron flux with increasing separation.

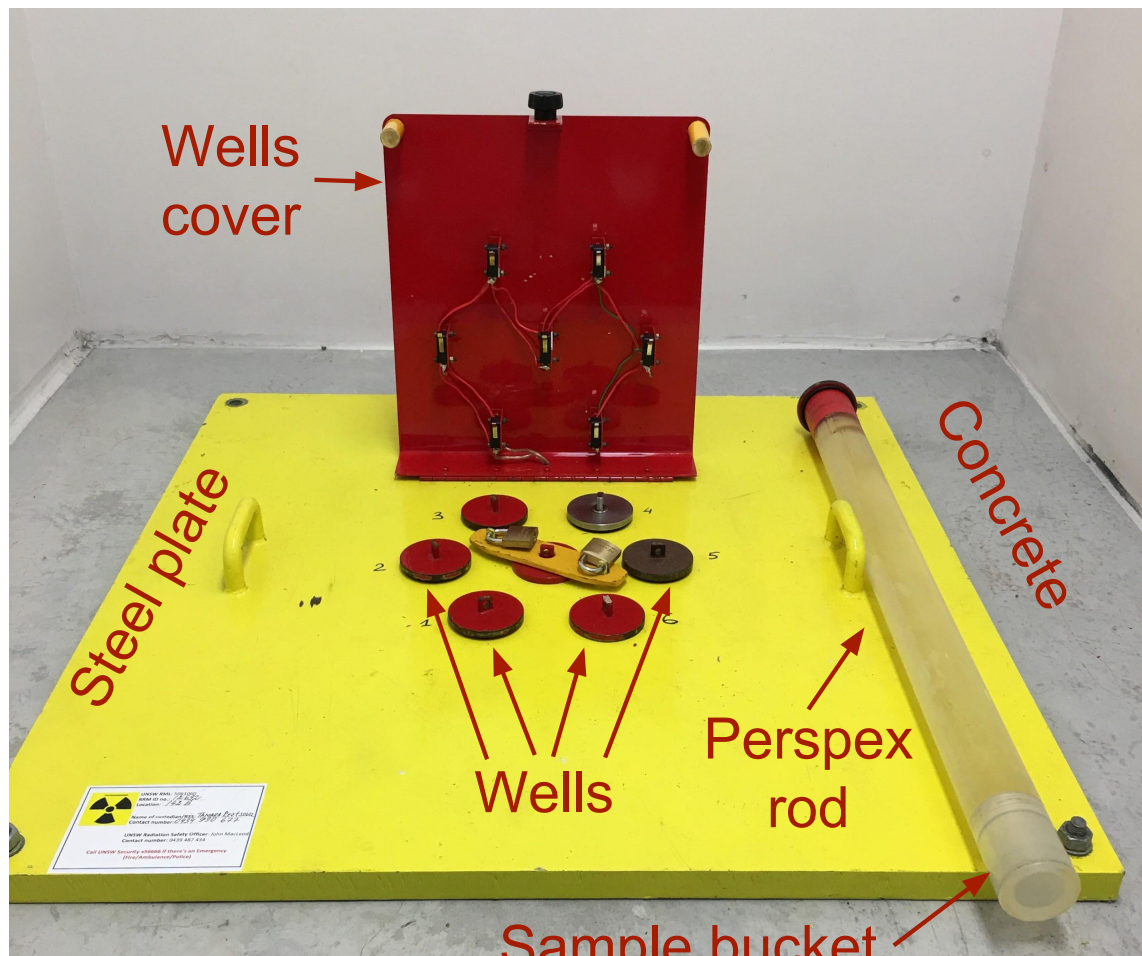
The In samples are discs of indium metal 30 mm in diameter, glued onto cardboard backing for increased rigidity. The Ag samples are hollow cylinders 20 mm in diameter and 40 mm high. For neutron irradiation each sample is placed in a small perspex bucket which is screwed onto the end of a perspex rod, and is lowered into an irradiation well for the required time. The irradiations are timed with an electronic timer and a stop watch is available to measure the time between removing a sample from the moderator and commencing counting on the sample.

4.2 Detection and Counting

The radiation detection apparatus consists of two types of Geiger-Muller (GM) tube: the end-window GM tube is used for counting the disc In specimens while the thin-walled tube is used for the cylindrical Ag samples. Both tubes are fragile and should be treated with care. They should be operated at the voltages indicated on each tube. The high voltage to operate the tubes is supplied by the GM-Radiation Counter, which also houses the computer interface which allows computer measurement of the count rates.



(a)



(b)

Figure 1: (a) Schematic diagram of the neutron moderator and (b) the exterior of the actual neutron moderator.

5 EXPERIMENTAL

5.1 WARNINGS!

- (i) The 20 GBq Am-241/Be source is the strongest radioactive source used in the laboratory. It emits low energy γ -rays as well as neutrons. The best protection from radiation is distance, so spend as little time as possible near the source. To encourage this an alarm sounds when the door to the neutron irradiation facility is open. Before going down to the moderator facility **make sure that a demonstrator switches off the security alarm** in the neutron moderator room!
- (ii) Before lowering a sample into the moderator ensure that the sample bucket is properly screwed onto the moderating rod (do not over tighten, otherwise the ‘Perspex’ will crack). **Take care not to drop the rods and buckets as they crack easily.**
- (iii) The **In** samples and the **Cd** and **Pb** discs are **all poisonous metals** and must only be **handled with gloves or tweezers**. Once irradiated, the ‘Perspex’ rods and buckets should be handled with gloves and the samples with tweezers.
- (iv) To minimize the number of fast neutrons escaping from the irradiation wells, **all four ‘Perspex’ rods** (containing samples, or empty) **must always be replaced in the moderator**. The moderator alarm will sound unless this is done.
- (v) The GM tubes require **high voltage** for operation. Take appropriate precautions and in particular make sure that the GM-Radiation Counter is **switched off** (switch on the back, left) when changing tubes.
- (vi) The end-window GM tube has a **very thin mica window** under the aluminium foil. Take good care not to poke the tweezers (or other objects) through the foil.

5.2 Experiments

NOTE: At the end of each afternoon please leave two In discs, in separate buckets, in the moderator, for the next group of students.

* * * * *

Check that the end window Geiger-Müller (GM) tube is connected to the GM-Radiation Counter and switch it on (switch on back, left), see figure 2. Switch on the computer, start ‘STX x64’ software from the desktop (figure 3) and set the tube voltage to 950V. Without any radioactive sources nearby, measure the room background for 15-20 minutes (w. preset time = 300s).

You can save your data in ‘My Documents/Student data’ - create a ‘New Folder’ here with your surname.

Experiment 1: Half-life of In isotope

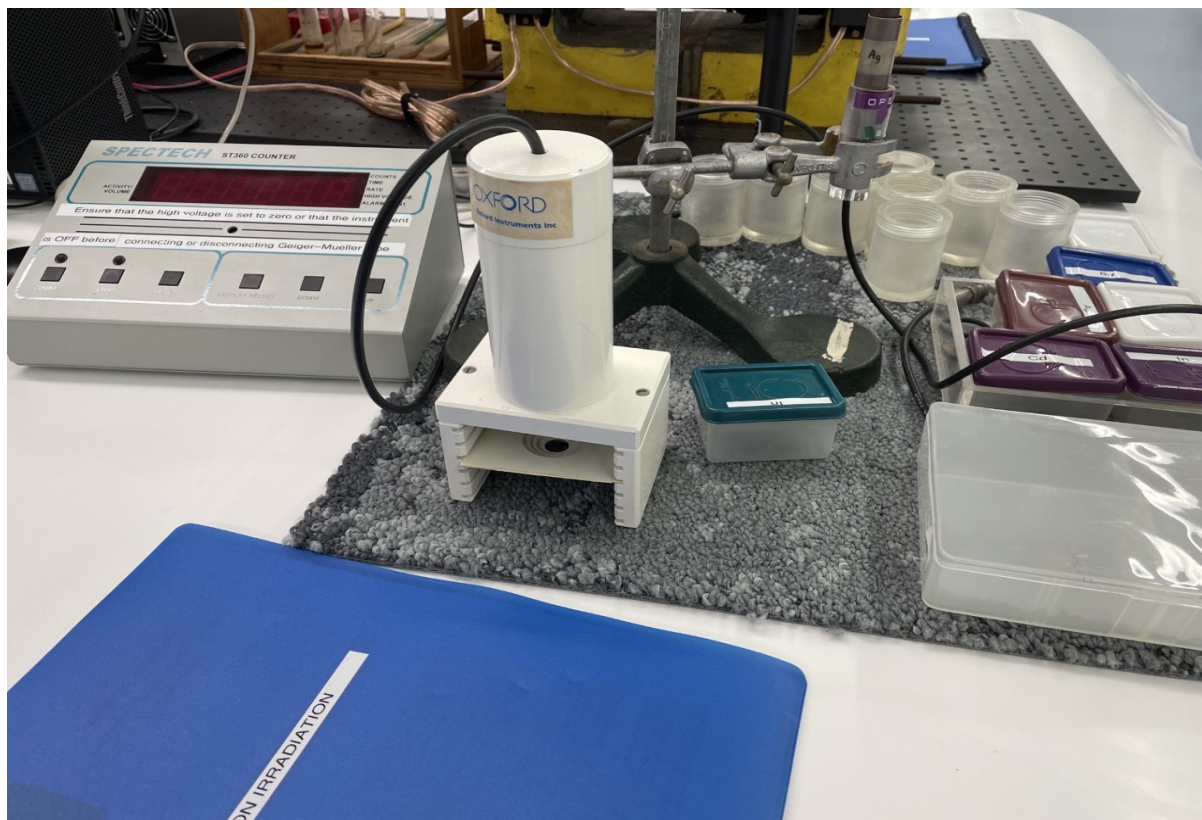


Figure 2: Experiment setup.

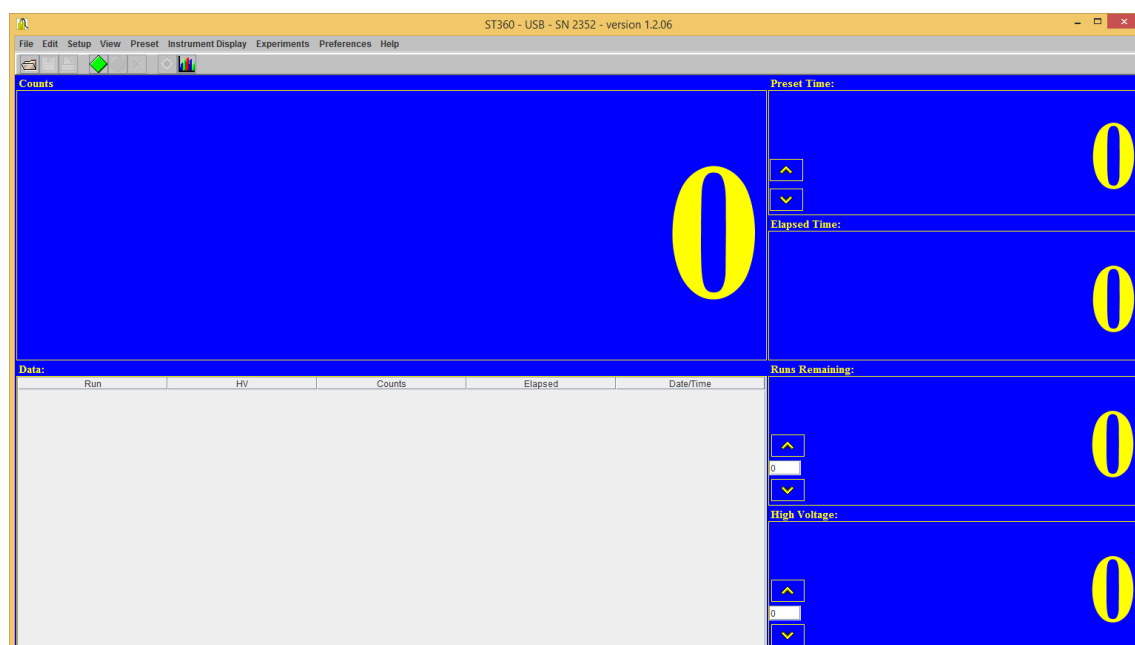


Figure 3: STX x64 software interface.

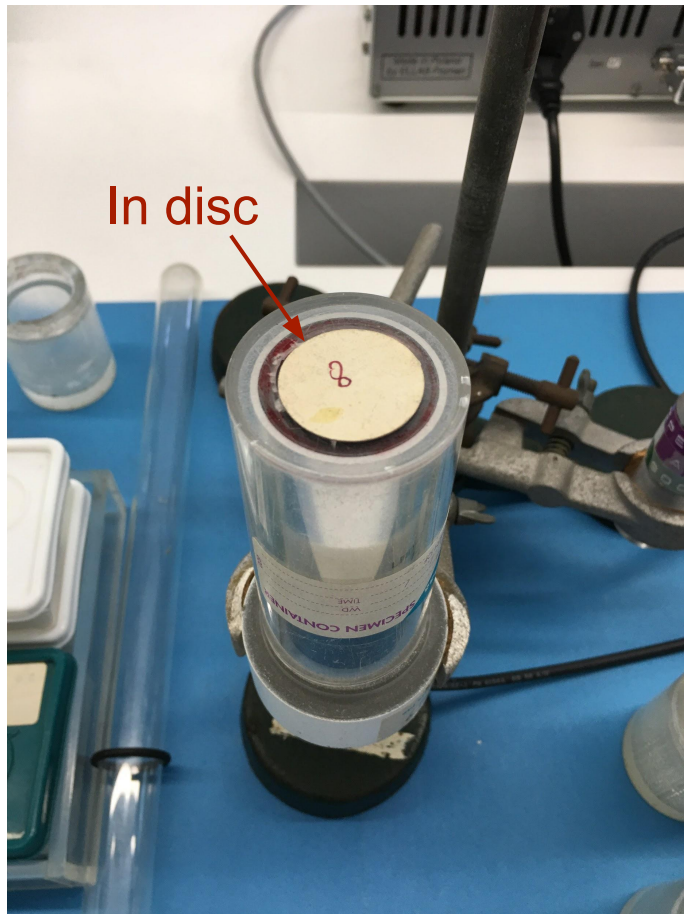


Figure 4: In disc and the GM tube.

Noting which well it was in, remove an indium disc (which has been irradiated at least overnight) from the moderator, figure 1, and place it centrally on top of the GM tube as shown in figure 4.

Note: Don't leave a well empty. Insert the extra perspex rod in the vacant well.

Start counting (preset time = 300s) 2 minutes (measured using stopwatch) after removing the sample from the moderator and count for at least one hour.

* * * * *

In the meantime put four inactive In discs into four **separate** buckets and lower all four into the irradiation wells. Note the time when the irradiation commences. These discs are for use in Experiment 2, and should be irradiated for times of about 90, 120, 150 and 180 minutes.

While waiting, you may do Experiment 4.

* * * * *

1. Correct the counts for room background and calculate the error for each point (see Appendix). Fit with an exponential decay curve (using 'Half Life' in the 'Neutron Experiment' software package) to find the half-life of the In isotope.
2. Get a hard copy of the data, together with the curve of best fit, using log (counts) vs. linear (time) scales.
3. Comment on your results.

Question 1: Which In isotope's half-life have you measured ? (see Ref.1, Appendix D)
How does your half-life compare with the normally accepted value?

Experiment 2: Growth of In activity

NOTE: This experiment is best divided over two afternoons.

* * * * *

Set the preset time to 600s. In separate buckets irradiate single In discs for **measured** times of about 10, 25, 40, 60, 90, 120, 150 and 180 minutes. To save time, the irradiations should be carried out simultaneously in all six wells, make sure to note, however, in which well a given disc is irradiated since the neutron flux varies from well to well (see Table II for flux ratios).

At the appropriate time remove a disc from the moderator, and place it on top of the GM tube. Start counting each sample 2 minutes (stopwatch!) after removing from the moderator and count for 600s.

- Correct the counts for room background and neutron flux and, using the half-life from Experiment 1, fit your experimental values of counts (remember to include errors!) versus irradiation time to find the saturation count S.
- Get a hard copy of the data and the best fit curve, with linear scales on both axes (make sure the saturation line at S is included). Compare the saturation count with the sum of the first two counts from Experiment 1 (corrected for well position - Table 2) and comment on your results.

Question 2: After removing the In sample from the moderator why should you wait at least 1.5 minutes before starting to count?

Experiment 3: Half-life of Ag isotope

Use the thin-walled GM tube (switch off HV before changing tubes; note different operating voltage) and set the preset time to 30s. Measure the background for at least 5 minutes.

Irradiate a silver cylinder for about 15 minutes, then slip it over the detector and commence counting **as soon as possible** after removing from the moderator. Count 30 s counts for a total of 7.5 minutes.

- Subtract room background and fit an exponential decay curve to the counts for the **last 5 minutes** (i.e. leave out the first five readings) to find the half-life and the best fit curve.
- On a log-linear graph, plot all (**including the first five**) experimental counts, with error bars, as a function of time, together with the best-fit curve. Extrapolate the best-fit curve back to zero time and comment on your results.

Question 3: Which Ag isotope's half-life have you measured and how does your value compare with that normally accepted?

Question 4: Why are the first few points well off the curve of best fit?

Question 5: How could you determine the half-life of the Ag isotopes more precisely?

Experiment 4: Effect of Shielding

Irradiate an **inactive** In disc for 10 minutes, cool off for 2 minutes and then count for 300 s. Carry out 3 more 10 min irradiations of an inactive In disc, **sandwiched between two shielding discs** of a a) lead, b) cadmium and c) indium, during the irradiation.

In each case cool off for 2 min and count the In disc only (**without the shields!**) for 300 s.

Question 6: Which metal is the best thermal neutron shield? Why? (Ref.1 or Ref.3)

Question 7: In experiment 2, why aren't all the In discs irradiated together, in the same bucket, and pulled out one at a time for counting at appropriate times?

Experiment 5: Optional

1. **Half-life of Cu isotope:** irradiate the copper disc sufficiently long to allow you to determine the half-life of a Cu isotope. Which isotope's half-life have you measured? Are other Cu isotopes formed?
2. **Cu content of alloys:** by irradiating with neutrons for a suitable time, find the percentage copper content of the brass disc and of the 20c coin. Estimate the errors in your content determination.

6 REFERENCES

1. Friedlander G. et al, "Nuclear and Radiochemistry" (1981) - 3rd edition.
2. Krane K.S., "Introductory Nuclear Physics" (1988)
3. Lederer C.M., Hollander J.M. and Perlman I., "Table of Isotopes" (1968) - 6th edition.

Table 1: Thermal neutron capture cross sections (σc) of some nuclides
(* 1 barn = 10^{-28} m² ≈ area of a nucleus)

Nuclide	Natural abundance (%)	σc (barn)*	Product Isotope	Main radiation emitted by product
1_1H	99.99	0.332	2_1H	Stable
$^{12}_6C$	98.89	0.0034	$^{13}_6C$	Stable
$^{107}_{47}Ag$	51.35	35	$^{108}_{47}Ag$	β^- : 1.64 MeV, 97.5%
$^{109}_{47}Ag$	48.65	89	$^{110}_{47}Ag$	β^- : 2.87 MeV, 95.5%
$^{115}_{49}In$	95.7	45	$^{116}_{49}In$	β^- : 3.33 MeV, 99%
$^{115}_{49}In$	95.7	154	$^{116m}_{49}In$	β^- : 1.01 MeV, 49% 0.87 MeV, 40% 0.60 MeV, 11%

Table 2: Neutron flux ratios in the six moderator wells

Well position	Flux ratio
1	1.1
2	1.01
3	1.03
4	1.00
5	1.08
6	1.18

Appendix

(i) For two independent measured quantities, A and B, obeying Poisson statistics

(a) if we form the sum/difference

$$SD = A \pm B$$

the statistical error is given by:

$$\sigma(SD) = (\sigma^2(A) + \sigma^2(B))^{1/2}$$

(b) If we form the product/quotient

$$PQ = A_x B$$

the statistical error is given by:

$$\frac{\sigma(PQ)}{PQ} = \left(\left(\frac{\sigma(A)}{A} \right)^2 + \left(\frac{\sigma(B)}{B} \right)^2 \right)^{1/2}$$

(ii) If we count n counts in a time t the statistical error in the count **rate**, N, is given by

$$\frac{\sigma(N)}{N} = \left(\left(\frac{\sigma(n)}{n} \right)^2 + \left(\frac{\sigma(t)}{t} \right)^2 \right)^{1/2}$$

assuming $\sigma(t)/t$ is negligible we get

$$\frac{\sigma(N)}{N} = \frac{\sigma(n)}{n} = \frac{1}{\sqrt{n}}$$

for random events.

FOLDER CONTENTS

Neutron Irradiation

1. **Friedlander G. et al, “Nuclear and radiochemistry”, 3rd ed. (1981)** - extracts from Appendix D, “Tables of Nuclides by Shirley V. S. and Lederer C. M.
2. Krane K. S., “Introductory nuclear physics” (1988) - extracts:
 - §5.1 The shell model
 - §12.1 Neutron sources
 - §12.2 Absorption and moderation of neutrons
3. **Friedlander G. et al, “Nuclear and radiochemistry”, 3rd ed. (1981)** - extracts:
 - Cross sections
 - Compound nucleus model
 - Slowing down of neutrons
 - Neutron sources

Appendix D

Table of Nuclides

V. S. Shirley and C. M. Lederer
Isotopes Project
Lawrence Berkeley Laboratory

This table presents properties of nuclides, both stable and radioactive, adopted from the seventh edition of the *Table of Isotopes* (L1). The data are based on experimental results reported in the literature, with the cutoff date varying from January to December, 1977. (The earliest date refers to the lightest nuclides, and vice versa.) Most mass excesses are from the 1977 Atomic Mass Evaluation (W1), with some recent experimental values added. For a few of the very unstable nuclides for which no values were reported in the 1977 Atomic Mass Evaluation, estimates are taken from the tables of W. D. Myers (M1). Natural isotopic abundances (H1) and neutron cross sections (H2) are taken from compilations by N. E. Holden. For other references, original data, and information on the data measurements the reader is referred to L1.

Column 1, Nuclide

Nuclides are listed in order of increasing atomic number Z , and are subordered by increasing mass number A . All isotopic species with half lives longer than about 1 s are included, as are the few shorter-lived ground states, fission isomers, and "historic" isomers (e.g., $^{24}\text{Na}^m$). Isotopes in L1 with ambiguous or very uncertain assignments, or whose assignments are probably in error (class "G"), have been omitted. Also not included are those nuclides identified in nuclear reactions, but for which radioactive decay has not been observed (class "R" in L1). Isomeric states are denoted by the conventional symbols m , m_1 , m_2 , and so on. Identical mass assignments (with no m) for several species indicate that the relative positions of the isomers are unknown.

Column 2, Abundance and Half Life

Half lives are given in plain type, natural isotopic abundances in italics. Half lives are rounded so that the uncertainty is ≤ 5 units in the last place. A question mark following the half life indicates that the assignment of the

half life (and other measured decay properties) to the listed values of Z and A is rather uncertain (nuclides with class "F" in L1).

Abundances (in atom percent) are also rounded to an uncertainty of ≤ 5 units in the last place, although the uncertainties are not well known. (Note that, because of the rounding, the abundances for an element do not always add to exactly 100 percent.) For additional information on abundances observed in specific sources and for variations in abundances the reader is referred to L1 and H1.

Column 3, Decay Mode

β^-	negative beta decay.
β^+ , EC or EC, β^+	both positive beta decay and electron capture have been experimentally shown to occur, with the first-named mode dominant from theoretical considerations; percentage branchings are given when known, e.g., EC 90%, β^+ 10%.
β^+ or EC	β^+ (or EC) has been observed or inferred from genetic relationships, with the other decay mode probably ≤ 1 percent from theoretical considerations.
$\beta^+ + EC$ or EC + β^+	the first-named mode has been observed or inferred from genetic relationships; the second mode is probably ≥ 1 percent from theoretical considerations.
IT	isomeric transition (γ -ray and conversion-electron decay).
α	alpha decay.
SF	spontaneous fission (listed only if branching by this mode is ≥ 1 percent).
p	direct proton decay ($^{53}\text{Co}^m$).
$\beta^- \beta^-$	double negatron emission.
$\beta^- n$	"delayed" neutron emission following β^- decay to unbound states. Other delayed particle-emission modes include $\beta^- \alpha$, $\beta^+ p$, $\beta^+ \alpha$, $\beta^+ SF$, and so on.

Decay modes inferred from the means of production are enclosed in square brackets. For nuclides that decay by more than one mode, branching ratios are given if known; they are rounded so that the uncertainty is ≤ 5 units in the last place.

Column 4, Mass Excess Δ

Mass excesses are given in MeV, with $\Delta(^{12}\text{C})$ defined as zero. Values are quoted to the number of significant figures implied in W1, except that very precise values have been rounded to the nearest keV. An appended *s* denotes a mass excess estimated from systematic considerations.

Column 5, Spin J and Parity π

Spin and parity assignments without parentheses are definite; assignments in parentheses are probable. Values enclosed in square brackets are inferred from systematics.

Column 6, Neutron Cross Section σ_n

Neutron cross sections are given in barns ($b = 10^{-24} \text{ cm}^2$), and, in the absence of additional notation, refer to thermal-neutron capture cross sections [$\sigma_c = \sigma(n, \gamma)$] at a neutron velocity of 2200 m s^{-1} ($E = 0.0253 \text{ eV}$, or $T = 293 \text{ K}$). A superscript sc following the value indicates a cross-section measurement with "subcadmium" neutrons, those with energy $\leq 0.5 \text{ eV}$ to which a cadmium absorber is "opaque"; the superscript rs refers to "reactor spectrum" neutrons, with an energy spectrum that is not well defined but that is approximately characteristic of a "thermal" irradiation position in a reactor. The subscripts f (fission), a (total absorption, $n\alpha$, and np identify cross sections other than the capture cross section. The symbols m and g as subscripts stand for "metastable" and "ground," and are used wherever separate cross sections are reported for capture to ground and isomeric states. For those cases for which a single total cross section includes both direct capture and indirect capture via the isomeric states, the subscript g + m is used. For additional details the reader is referred to L1.

To use the table for the calculation of the rate of a nuclear reaction in a sample placed in a nuclear reactor, it must be realized that the magnitude of the flux of neutrons at any point in a reactor is given by the expression

$$n \int_0^\infty v P(v) dv = n \bar{v}, \quad (\text{D-1})$$

where n is the density of neutrons at that point, $P(v) dv$ is the probability that a neutron will have a velocity between v and $v + dv$, and \bar{v} is the average velocity. If the neutron-reaction cross section is in the $1/v$ region (see chapter 4, section D), then the rate of the reaction is

$$R = N n v_0 \sigma_0, \quad (\text{D-2})$$

where N is the number of target nuclei in the sample and σ_0 is the cross section at v_0 .

REFERENCES

- H1 N. E. Holden, "Isotopic Composition of the Elements and Their Variation in Nature: A Preliminary Report," Brookhaven National Laboratory Report No. BNL-NCS-50605, 1977 (unpublished, available from Nat. Tech. Info. Service, Springfield, VA).
- H2 N. E. Holden, private communication to C. M. Lederer and V. S. Shirley, 1977.

TABLE OF NUCLIDES 609

- L1 C. M. Lederer and V. S. Shirley (Eds.); E. Browne, J. M. Dairiki, and R. E. Doeblir (principal authors); A. A. Shihab-Eldin, L. J. Jardine, J. K. Tuli, and A. B. Buryn (authors), *Table of Isotopes*, 7th ed., Wiley, New York, 1978.
- M1 W. D. Myers, *Droplet Model of Atomic Nuclei*, IFI/Plenum, New York, 1977; see also *At. Data Nucl. Data Tables* 17, 474 (1976).
- W1 A. H. Wapstra and K. Bos, "The 1977 Atomic Mass Evaluation," *At. Data Nucl. Data Tables* 19, 175 (1977); *At. Data Nucl. Data Tables* 20, 1 (1977); Errata: *At. Data Nucl. Data Tables* 20, 126 (1977).

TABLE OF NUCLIDES

Z	Nuclide El	A	Abundance or $t_{1/2}$	Decay Mode	Δ (MeV)	$J\pi$	$\sigma_n(b)$
0	n	1	10.6 m	β^- , no γ	8.071	1/2+	
1	H	1	99.995%		7.289	1/2+	0.332
		2	0.0148%		13.136	1+	5.2×10^{-4}
		3	12.33 y	β^- , no γ	14.950	1/2+	$<6 \times 10^{-6}$ sc
2	He	3	$1.38 \times 10^{-4}\%$		14.931	1/2+	5.33×10^3 np
		4	99.99986%		2.425	0+	
		6	0.808 s	β^- , no γ	17.597	0+	
		8	0.122 s	β^- , β^-n 12%	31.609	0+	
3	Li	6	7.5%		14.087	1+	942 na
		7	92.5%		14.908	3/2-	0.045 rs
		8	0.84 s	$\beta^-2\alpha$	20.947	2+	
		9	0.178 s	β^- , $\beta^-n2\alpha$ 35%	24.955	(3/2)-	
		11	8.5 ms	β^- , β^-n 61%	40.94		
4	Be	7	53.3 a	EC	15.770	3/2-	5×10^4 rs
		9	100%		11.348	3/2-	0.008
		10	1.6×10^6 y	β^- , no γ	12.608	0+	<0.001 rs
		11	13.8 s	β^- , β^-a 3%	20.176	1/2+	
		12	11.4 ms	β^- , β^-n	25.03	0+	
5	B	8	0.769 s	$\beta^+2\alpha$	22.922	2+	
		10	19.8%		12.052	3+	3838 na
		11	80.2%		8.668	3/2-	0.005 rs
		12	20.4 ms	β^- , $\beta^-3\alpha$ 1.6%	13.370	1+	
		13	17.4 ms	β^- , β^-n 0.28%	16.562	3/2-	
		14	16 ms	β^-	23.657	2-	
6	C	9	0.1265 s	$\beta^+p2\alpha$	28.912	(3/2-)	
		10	19.2 s	β^+	15.703	0+	
		11	20.38 m	β^+ 99.76%, EC 0.24%, no γ	10.650	3/2-	
		12	98.89%		0	0+	0.0034
		13	1.11%		3.125	1/2-	9×10^{-4}
		14	5730 ,	β^- , no γ	3.020	0+	$<1 \times 10^{-6}$ rs
		15	2.449 s	β^-	9.873	1/2+	
		16	0.75 s	β^-n >98.8%	13.693	0+	
7	N	12	11.0 ms	$\beta^+, \beta^+3\alpha$ 3.5%	17.338	1+	
		13	9.96 m	β^+ , no γ	5.346	1/2-	
		14	99.63%		2.863	1+	1.82 sc np
		15	0.366%		0.102	1/2-	4×10^{-5} rs
		16	7.13 s	β^- , β^-a 0.0012%	5.682	2-	
		17	4.17 s	β^- , β^-n 95%	7.870	1/2-	
		18	0.63 s	β^-	13.274	0,1,2-	
8	O	13	8.9 ms	β^+p	23.105	3/2-	
		14	70.60 s	β^+	8.008	0+	
		15	122 s	β^+ 99.89%, EC 0.11%, no γ	2.855	1/2-	
		16	99.76%		-4.737	0+	1.8×10^{-4} rs
		17	0.038%		-0.810	5/2+	0.235 na
		18	0.204%		-0.783	0+	1.6×10^{-4}
		19	26.9 s	β^-	3.331	5/2+	
		20	13.5 s	β^-	3.799	0+	
9	F	17	64.5 s	β^- , no γ	1.952	5/2+	
		18	109.8 m	β^+ 96.9%, EC 3.1%, no γ	0.872	1+	
		19	100%		-1.487	1/2+	0.010 rs
		20	11.0 s	β^-	-0.017	2+	
		21	4.32 s	β^-	-0.047	5/2+	
		22	4.23 s	β^-	2.826	4+	
		23	2.2 s	β^-	3.35	(5/2)+	
10	Ne	17	0.109 s	β^+p	16.478	1/2-	
		18	1.67 s	β^+	5.319	0+	
		19	17.3 s	β^+ 99%, EC 0.102%	1.751	1/2+	
		20	90.5%		-7.043	0+	0.038 rs
		21	0.27%		-5.733	3/2+	0.7 rs

TABLE OF NUCLIDES

Z	Nuclide El	A	Abundance or $t_{1/2}$	Decay Mode	$\Delta(\text{MeV})$	$J\pi$	$\sigma_n(\text{b})$
10	Ne 22		9.22%		-8.026	0+	0.05 ^{rs}
	23	37.6 s	β^-		-5.155	5/2+	
	24	3.38 m	β^-		-5.949	0+	
	25	0.60 s	β^-		-2.15	(1/2)+	
11	Na 20	0.446 s	$\beta^+, \beta^+ \alpha$ 21%		6.844	2+	
	21	22.47 s	β^+		-2.186	3/2+	
	22	2.602 y	β^+ 90.5%, EC 9.5%		-5.184	3+	3.2×10^4
	23	100%			-9.530	3/2+	0.43 ^m 0.10 ^g
	24	15.02 h	β^-		-8.418	4+	
	24m	20.2 ms	IT, β^- (weak)		-7.945	1+	
	25	60 s	β^-		-9.357	5/2+	
12	26	1.07 s	β^-		-6.888	3+	
	27	0.30 s	$\beta^-, \beta^- n$ 0.08%		-5.63	3/2, 5/2+	
	28	31 ms	$\beta^-, \beta^- n$ 0.6%		-1.13	1+	
	29	43 ms	$\beta^-, \beta^- n$ 15%		2.66		
	30	54 ms	$\beta^-, \beta^- n$ 33%		8.38		
	31	17 ms	$\beta^-, \beta^- n$ 30%		10.61		
	32	14.5 ms	β^-		16.41		
	33	0.02 s	β^-				
	21	123 ms	$\beta^+ p$		10.912	5/2+	
	22	3.86 s	β^+		-0.394	0+	
13	23	11.3 s	β^+		-5.471	3/2+	
	24	78.99%			-13.931	0+	0.053 ^{rs}
	25	10.00%			-13.191	5/2+	0.18 ^{rs}
	26	11.01%			-16.212	0+	0.038
	27	9.46 m	β^-		-14.585	1/2+	0.15 ^{rs}
	28	21.0 h	β^-		-15.016	0+	
	29	1.4 s	β^-		-10.75	(3/2+)	
	30	1.2 s	β^-		-9.79 s	0+	
	23	0.47 s	$\beta^+, \beta^+ p$		6.768		
	24	2.07 s	$\beta^+, \beta^+ \alpha$ 0.0077%		-0.052	4+	
14	24m	0.13 s	IT 93%, β^+ 7%, $\beta^+ \alpha$		0.387	1+	
	25	7.18 s	β^+		-8.913	5/2+	
	26	7.2×10^5 y	β^+ 82%, EC 18%		-12.208	5+	
	26m	6.36 s	β^+ , no γ		-11.979	0+	
	27	100%			-17.194	5/2+	0.231
	28	2.24 m	β^-		-16.848	3+	
	29	6.6 m	β^-		-18.212	5/2+	
	30	3.69 s	β^-		-15.89	(2,3)+	
	31	0.64 s	β^-		-15.10	5/2, 3/2+	
	25	0.22 s	$\beta^+, \beta^+ p$		3.824	3/2, 5/2+	
15	26	2.21 s	β^+		-7.143	0+	
	27	4.13 s	β^+		-12.385	5/2+	
	28	92.23%			-21.491	0+	0.17 ^{rs}
	29	4.67%			-21.894	1/2+	0.10 ^{rs}
	30	3.10%			-24.432	0+	0.108
	31	2.62 h	β^-		-22.949	3/2+	0.5 ^{rs}
	32	≈ 650 y	β^- , no γ		-24.092	0+	
	33	6.2 s	β^-		-20.57		
	34	2.8 s	β^-		-19.85	0+	
	28	270 ms	β^+		-7.160	3+	
16	29	4.1 s	β^+		-16.949	1/2+	
	30	2.50 m	β^+ , EC		-20.204	1+	
	31	100%			-24.440	1/2+	0.18 ^{rs}
	32	14.28 d	β^- , no γ		-24.305	1+	
	33	25.3 d	β^- , no γ		-26.337	1/2+	
	34	12.4 s	β^-		-24.55	1+	
	35	47 s	β^-		-24.94	(1/2, 3/2)+	
17	29	0.19 s	$\beta^+, \beta^+ p$		-3.16	5/2+	
	30	1.2 s	β^+		-14.062	0+	
	31	2.6 s	β^+		-19.044	1/2+	
	32	95.02%			-26.015	0+	0.53 ^{rs}
	33	0.75%			-26.586	3/2+	0.09 ^{rs}
18	34	4.21%			-29.931	0+	0.24 ^{rs}
	35	87.4 d	β^- , no γ		-28.846	3/2+	

TABLE OF NUCLIDES

Z	Nuclide	Abundance or $t_{1/2}$	Decay Mode	$\Delta(\text{MeV})$	$J\pi$	$\sigma_n(b)$
	El	A				
26	Fe 54	5.8%		-56.251	0+	2.2 ^{rs}
	55	2.7 y	EC,no γ	-57.479	3/2-	
	56	91.8%		-60.604	0+	2.6 ^{rs}
	57	2.15%		-60.179	1/2-	2.4 ^{rs}
	58	0.29%		-62.152	0+	1.14
	59	44.6 d	β^-	-60.661	3/2-	
	60	3×10^5 y	β^-	-61.437	0+	
	61	6.0 m	β^-	-59.01	(3/2)-	
	62	68 s	β^-	-58.86	0+	
27	Co 53	0.26 s	$\beta^+, \text{no } \gamma$	-42.640	[7/2-]	
	53m	0.25 s	$\beta^+ \approx 98.5\%, p \approx 1.5\%$	-39.453	[19/2-]	
	54	193.2 ms	$\beta^+, \text{no } \gamma$	-48.010	0+	
	54m	1.46 m	β^+	-47.811	(7+)	
	55	17.5 h	$\beta^+ 77\%, \text{EC } 23\%$	-54.024	7/2-	
	56	78.8 d	EC 81%, $\beta^+ 19\%$	-56.037	4+	
	57	271 d	EC	-59.342	7/2-	
	58	70.8 d	EC 85.00%, $\beta^+ 15.00\%$	-59.844	2+	1.9×10^3
	58m	9.2 h	IT	-59.819	5+	1.4×10^5
	59	100%		-62.226	7/2-	
	60	5.271 y	β^-	-61.647	5+	2.0 ^{sc}
	60m	10.5 m	IT 99.75%, $\beta^- 0.25\%$	-61.588	2+	58 ^{sc}
	61	1.65 h	β^-	-62.897	7/2-	
	62(g)	1.50 m	β^-	-61.430	(2)+	
	62(m)	13.9 m	β^-	-61.408	(5)+	
	63	27.5 s	β^-	-61.850	7/2, 5/2-	
	64	0.3 s	β^-	-59.791	(1+)	
28	Ni 53	0.05 s	$[\beta^+], \beta^+ p$	-29.41	[7/2-]	
	56	6.10 d	EC	-53.902	0+	
	57	36.0 h	EC 60%, $\beta^+ 40\%$	-56.077	3/2-	
	58	68.3%		-60.224	0+	4.6 ^{rs}
	59	7.5×10^4 y	EC 99+%, $\beta^+ 1.5 \times 10^{-5}\%, \text{no } \gamma$	-61.153	3/2-	92 _c
	60	26.1%		-64.470	0+	2.8 ^{rs}
	61	1.13%		-64.219	3/2-	2 ^{rs}
	62	3.59%		-66.745	0+	14.2
	63	100 y	$\beta^-, \text{no } \gamma$	-65.513	1/2-	23 ^{rs}
	64	0.91%		-67.098	0+	1.49
	65	2.520 h	β^-	-65.124	5/2-	24 ^{sc}
	66	54.8 h	$\beta^-, \text{no } \gamma$	-66.021	0+	
	67	18 s	β^-	-63.47		
29	Cu 58	3.20 s	β^+	-51.662	1+	
	59	82 s	β^+	-56.352	3/2-	
	60	23.4 m	$\beta^+ 93\%, \text{EC } 7\%$	-58.343	2+	
	61	3.41 h	$\beta^+ 62\%, \text{EC } 38\%$	-61.981	3/2-	
	62	9.73 m	$\beta^+ 97.8\%, \text{EC } 2.2\%$	-62.796	1+	
	63	69.2%		-65.578	3/2-	4.4
	64	12.70 h	EC 41%, $\beta^+ 19\%, \beta^- 40\%$	-65.423	1+	
	65	30.8%		-67.262	3/2-	2.17
	66	5.10 m	β^-	-66.257	1+	140 ^{sc}
	67	61.9 h	β^-	-67.305	3/2-	
	68	31 s	β^-	-65.39	1+	
	68m	3.8 m	IT 86%, $\beta^- 14\%$	-64.66	(6-)	
	69	3.0 m	β^-	-65.94	(3/2)-	
	70(g)	5 s	β^-	-63.39	1+	
	70(m)	47 s	β^-	-63.25	(5-)	
30	Zn 57	0.04 s	$[\beta^+], \beta^+ p$	-32.61	[7/2-]	
	60	2.4 m	$\beta^+ \approx 97\%, \text{EC } \approx 3\%$	-54.184	0+	
	61	89.1 s	$\beta^+ \approx 99\%, \text{EC } \approx 1\%$	-56.58	3/2-	
	62	9.2 h	EC 93%, $\beta^+ 7\%$	-61.169	0+	
	63	38.1 m	$\beta^+ 93\%, \text{EC } 7\%$	-62.211	3/2-	
	64	48.6%		-66.001	0+	0.78
	65	244.1 d	EC 98.54%, $\beta^+ 1.46\%$	-65.910	5/2-	
	66	27.9%		-68.898	0+	1 ^{rs}

TABLE OF NUCLIDES

Z	Nuclide El	A	Abundance or $t_{1/2}$	Decay Mode	Δ (MeV)	$J\pi$	$\sigma_n(b)$
30	Zn	67	4.10%		-67.880	5/2-	7^{rs}
		68	18.8%		-70.006	0+	0.81_g
		69	56 m	β^-	-68.417	1/2-	
		69m	14.0 h	IT 99.9%, β^- 0.033%	-67.978	9/2+	
		70	0.62%		-69.560	0+	0.09_g
		71	2.4 m	β^-	-67.324	1/2-	
		71m	3.9 h	β^-	-67.167	(9/2)+	
		72	46.5 h	β^-	-68.134	0+	
		73	24 s	β^-	-65.03		
		74	95 s	β^-	-65.67	0+	
		75	10.2 s	β^-	-62.46 s		
		76	5.7 s	β^-	-62.55	0+	
		77	1.4 s	β^-	-58.91 s		
		79	2.6 s?	β^-n			
	31	Ca	118 ms	β^+	-51.77 s	(0+)	
		63	32 s	β^+	-56.69	3/2, 5/2-	
		64	2.62 m	β^+ +EC	-58.836	0+	
		65	15.2 m	β^+ 86%, EC 14%	-62.654	3/2-	
		66	9.4 h	β^+ 56.5%, EC 43.5%	-63.723	0+	
		67	78.3 h	EC	-66.878	3/2-	
		68	68.1 m	β^+ 90%, EC 10%	-67.085	1+	
		69	60.1%		-69.322	3/2-	1.7
		70	21.1 m	β^- 99.8%, EC 0.2%	-68.905	1+	
		71	39.9%		-70.142	3/2-	4.6
		72	14.10 h	β^-	-68.591	3-	
		73	4.87 h	β^-	-69.73	(3/2)-	
		74	8.1 m	β^-	-68.02	(4)-	
		74m	10 s	IT	-67.96	1+	
		75	2.10 m	β^-	-68.56	(3/2-)	
		76	27.1 s	β^-	-66.44	(3-)	
		77	13 s	β^-	-66.41 s		
		78	5.1 s	β^-	-63.68		
		79	3.0 s	β^-	-62.80		
		80	1.66 s	β^- , β^-n	-59.53 s		
		81	1.2 s	β^- , β^-n			
		82	0.60 s?	$[\beta^-]$, β^-n			
		83	0.31 s	$[\beta^-]$, β^-n			
32	Ge	64	64 s	β^+ +EC	-54.43	0+	
		65	31 s	β^+ +EC, $(\beta^++EC)p$ 0.013%	-56.41	3/2, 5/2-	
		66	2.3 h	EC 73%, β^+ 27%	-61.621	0+	
		67	19.0 m	β^+ 96%, EC 4%	-62.45	(1/2)-	
		68	288 d	EC, no γ	-66.972	0+	
		69	39.0 h	EC 64%, β^+ 36%	-67.096	5/2-	
		70	20.5%		-70.561	0+	3.2 ^{rs}
		71	11.2 d	EC, no γ	-69.906	1/2-	
		72	27.4%		-72.583	0+	$1.0^{rs}_{g,m}$
		73	7.8%		-71.294	9/2+	15 ^{rs}
		73m	0.50 s	IT	-71.227	1/2-	
		74	36.5%		-73.422	0+	0.4^{rs}_g
		75	82.8 m	β^-	-71.856	1/2-	
		75m	48 s	IT 99.97%, β^- 0.03%	-71.716	7/2+	
		76	7.8%		-73.214	0+	0.10^{rs}_m
		77	11.30 h	β^-	-71.214	7/2(+)	
		77m	53 s	β^- 80%, IT 20%	-71.055	1/2-	
		78	1.45 h	β^-	-71.76	0+	
		79	19 s?	β^-			
		79	42 s	β^-	-69.56	(1/2)-	
		80	29 s	β^-	-69.43	0+	
		81	10 s	β^-	-66.34 s		
		82	4.6 s	β^-	-65.99 s	0+	
		83	1.9 s	β^-	≈ 62.5 s		

TABLE OF NUCLIDES

Z	Nuclide El	A	Abundance or $t_{1/2}$	Decay Mode	$\Delta(\text{MeV})$	$J\pi$	$\sigma_n(b)$
45	Rh	108	6.0 m	β^-	-85.09		
		109	80 s	β^-	-85.11 s	(5/2,3/2)+	
		110	3 s	β^-	-82.8		
		110	28 s	β^-	-82.93		
		111	11 s	[β^-]	-82.53 s		
		112	4.6 s	β^-	-80.3 s		
		113	0.9 s	[β^-]			
		114	1.7 s?	β^-			
	Pd	97	3.3 m	$\beta^+ + \text{EC}$	-77.76 s		
		98	18 m	$\text{EC} + \beta^+$	-81.27 s	0+	
46		99	21.4 m	β^+, EC	-86.112	(5/2+)	
		100	3.6 d	EC	-85.230	0+	
		101	8.5 h	EC 93.6%, β^+ 6.4%	-85.428	(5/2)+	
		102	1.0%		-87.925	0+	5 ^{rs}
		103	17.0 d	EC	-87.478	5/2+	
		104	11.0%		-89.400	0+	
		105	22.2%		-88.422	5/2+	
		106	27.3%		-89.913	0+	0.28 _g 0.013 _m
		107	6.5×10^6 y	β^- , no γ	-88.371	5/2+	
		107m	21.3 s	IT	-88.156	11/2-	
47		108	26.7%		-89.523	0+	11 _g 0.19 _m ^{rs}
		109	13.43 h	β^-	-87.606	5/2+	
		109m	4.69 m	IT	-87.417	11/2-	
		110	11.8%		-88.335	0+	0.36 _g 0.02 _m ^{rs}
		111	22 m	β^-	-86.03	(5/2+)	
		111m	5.5 h	IT 71%, β^- 29%	-85.86	(11/2-)	
		112	21.1 h	β^-	-86.326	0+	
		113	1.5 m	β^- , no γ	-83.64 s		
		114	2.4 m	β^- , no γ	-83.76 s	0+	
		115	37 s	β^-			
48		116	14 s	β^-	-≈80.12 s	0+	
		117	5 s	[β^-]	-76.21 s	0+	
		118	3.1 s	β^-			
		99	1.8 m?	$\beta^+ + \text{EC}$	-76.51 s		
		100	2.3 m	$\beta^+ + \text{EC}$	-77.93		
		100	8 m?	$\beta^+ + \text{EC}$			
		101	10.8 m	$\beta^+ + \text{EC}$	-81.33 s	(9/2+)	
		102	13.0 m	$\beta^+ \approx 68\%$, EC $\approx 32\%$	-82.33	5+	
		102m	7.7 m	(β^+, EC) 51%, IT 49%	-82.32	2+	
		103	1.10 n	EC $\approx 58\%$, $\beta^+ \approx 42\%$	-84.80	7/2+	
49		103m	5.7 s	IT	-84.67	(1/2)-	
		104	69 m	β^+, EC	-85.150	5+	
		104m	33 m	(β^+, EC) 67%, IT 33%		2+	
		105	41.3 d	EC 99.7%, $\beta^+ 9 \times 10^{-4}\%$	-87.075	1/2-	
		105m	7.2 m	IT 99.7%, EC 0.3%	-87.049	(7/2)+	
		106	24.0 m	(EC, β^+) $\approx 99\%$, $\beta^- \approx 1\%$	-86.929	1+	
		106m	8.5 d	EC	-86.841	6+	
		107	51.83%		-88.404	1/2-	37 _g 0.3 _m ^{sc}
		107m	44.3 s	IT	-88.311	7/2+	
		108	2.4 m	β^- 97.7%, EC 2.1%, β^+ 0.24%	-87.602	1+	
50		108m	127 y	EC + β^+ 91%, IT 9%	-87.492	6+	
		109	48.17%		-88.722	1/2-	88 _g 4 _m
		109m	39.8 s	IT	-88.634	7/2+	
		110	24.4 s	β^- 99.7%, EC 0.3%	-87.456	1+	
		110m	252 d	β^- 98.5%, IT 1.5%	-87.338	6+	80 _{g+m}
		111	7.45 d	β^-	-88.226	1/2-	3 ^{rs}
51		111m	65 s	IT 99.7%, β^- 0.3%	-88.166	(7/2+)	
		112	3.14 n	β^-	-86.620	2(-)	

TABLE OF NUCLIDES

Z	Nuclide El	A	Abundance or $t_{1/2}$	Decay Mode	Δ (MeV)	$J\pi$	$\sigma_n(b)$
47 Ag	113		1.15 m	β^-	-86.82		
	113		5.37 h	β^-	-87.040	$1/2(-)$	
	114		4.5 s	β^-	-85.16	$1+$	
	115		18 s	β^-			
	115		20 m	β^-	-84.91	(1/2-)	
	116		2.68 m	β^-	-82.62 s		
	116m		10.5 s	β^- ≈98%, IT ≈2%	-82.54 s		
	117		1.21 m	β^-	-82.24		
	117		5.3 s	β^-	-82.24		
	118		3.7 s	β^-	-80.21 s		
	118m		2.8 s	β^- 59%, IT 41%	-80.08 s		
	119		2.1 s	β^-	-79.31 s	(7/2+)	
	120		1.2 s	β^-	-≈78.0 s	(3+)	
	120m		0.32 s	β^- ≈63%, IT ≈37%	-≈77.8 s	(6-)	
	121		≤3 s	[β^-]			
	122		1.5 s	[β^-]	-≈70.5 s		
	123		0.39 s	[β^-], β^-n			
48 Cd	100		1.1 m	$\beta^+ + EC$	-73.43 s	0+	
	101		1.2 m	$\beta^+ + EC$	-75.53 s		
	102		5.5 m	EC, β^+	-79.43 s	0+	
	103		7.3 m	β^+, EC	-80.60		
	104		58 m	EC 99.2%, β^+ 0.8%	-83.57	0+	
	105		56.0 m	EC, β^+	-84.336	5/2+	
	106		1.25%		-87.131	0+	1 rs
	107		6.50 h	EC 99.77%, β^+ 0.23%	-86.987	5/2+	
	108		0.89%		-89.251	0+	1.2 rs
	109		453 d	EC	-88.540	5/2+	700 rs
	110		12.5%		-90.349	0+	11^{rs}_g 0.10 $^{rs}_m$
	111		12.8%		-89.254	1/2+	24 rs
	111m		48.6 m	IT	-88.858	11/2-	
	112		24.1%		-90.578	0+	2^{rs}_g
	113		12.2% 9×10^{15} y	β^- , no γ	-89.050	1/2+	1.98×10^4
	113m		14 y	β^- 99.9%, IT 0.1%	-88.787	11/2-	
	114		28.7%		-90.020	0+	0.30^{sc}_g 0.04^{sc}_m
	115		53.4 h	β^-	-88.093	1/2+	
	115m		44.8 d	β^-	-87.920	11/2-	
	116		7.5%		-88.718	0+	0.05^{sc}_g 0.025^{sc}_m
49 In	117		2.4 h	β^-	-86.416	1/2+	
	117m		3.4 h	β^-	-86.29	11/2-	
	118		50.3 m	β^- , no γ	-86.707	0+	
	119		2.7 m	β^-	-84.23	1/2+	
	119m		1.9 m	β^-	-84.08	11/2-	
	120		50.8 s	β^-	-83.98*	0+	
	121		12.8 s	β^-	-≈81.3 s		
	121		4.8 s	β^-	-≈81.3 s		
	122		5.8 s	β^-	-≈80.0 s	0+	
	124		0.9 s	β^-	-≈76.4 s	0+	
	104		1.5 m	$\beta^+ + EC$	-75.57 s		
	105		5.1 m	$\beta^+ + EC$	-79.34 s		
	105m		55 s?	IT?			
	106		5.3 m	$\beta^+ + EC$	-80.586	(3)	
	106		6.3 m	$\beta^+ + EC$			
	107		32.4 m	EC 65%, β^+ 35%	-83.50	9/2+	
	107m		50 s	IT	-82.82	1/2-	
	108		40 m	EC, β^+	-84.10	3+	
	108		58 m	EC, β^+	-84.13	(5,6+)	
	109		4.2 h	EC 94%, β^+ 6%	-86.524	9/2+	
	109m ₁		1.3 m	IT	-85.874	1/2-	
	109m ₂		0.21 s	IT	-84.41	(19/2+)	
	110		4.9 h	EC		7+	
	110		69 m	β^+, EC	-86.409	2+	
	111		2.83 d	EC	-88.405	9/2+	

TABLE OF NUCLIDES

Z	Nuclide El	A	Abundance or $t_{1/2}$	Decay Mode	$\Delta(\text{MeV})$	$J\pi$	$\sigma_n(\text{b})$
49 In	111m		7.6 m	IT	-87.869	$1/2^-$	
	112		14.4 m	β^- 44%, EC 34%, β^+ 22%	-88.000	1^+	
	112m		20.9 m	IT	-87.845	4^+	
	113		4.3%		-89.372	$9/2^+$	5_m
	113m		99.5 m	IT	-88.980	$1/2^-$	3_g
	114		71.9 s	β^- 98.1%, EC 1.9%, β^+ 0.004%	-88.576	1^+	
	114m		49.51 d	IT 96.7%, EC 3.3%	-88.386	5^+	
	115		95.7% $5.1 \times 10^{14} \text{ y}$	β^- , no γ	-89.541	$9/2^+$	91_{m2} 70_{m1} 41_g
	115m		4.49 h	IT 95%, β^- 5%	-89.205	$1/2^-$	
	116		14.10 s	β^-	-88.253	1^+	
	116m ₁		54.1 m	β^-	-88.126	5^+	
	116m ₂		2.16 s	IT	-87.963	8^-	
	117		42 m	β^-	-88.944	$9/2^+$	
	117m		1.93 n	β^- 53%, IT 47%	-88.629	$1/2^-$	
	118		5.0 s	β^-	-87.45	1^+	
	118		4.4 m	β^-	-87.37	(5)+	
	118		8.5 s	IT 98.5%, β^- 1.5%	-87.23	(8)-	
	119		2.1 m	β^-	-87.730	$9/2^+$	
	119m		18.0 m	β^- 95%, IT 5%	-87.419	$1/2^-$	
	120		4.4 s	β^-	-85.8	(5)+	
	120		3.0 s	β^-	-85.5	1^+	
	121		30.0 s	β^-	-85.842	$9/2^+$	
	121m		3.8 m	β^- 98.8%, IT 1.2%	-85.528	$1/2^-$	
	122		9.2 s	β^-	-83.4		
	122		1.5 s	β^-	-83.5	(1+)	
50 Sn	123(g)		6.0 s	β^-	-83.44	(9/2)+	
	123(m)		48 s	β^-	-83.12	(1/2)-	
	124		2.4 s	β^-			
	124		3.2 s	β^-	-81.10	(2+)	
	125		2.32 s	β^-	-80.50	(9/2)+	
	125		12.2 s	β^-			
	126		1.53 s	β^-	-77.90		
	127		1.3 s	β^-	-77.36		
	127		3.7 s	β^- , β^-n	-77.36		
	128		12 s?	[β^-], β^-n			
	129		2.5 s	β^- , β^-n			
	129		0.99 s	β^- , β^-n	-73.12		
	130		0.58 s	β^- , β^-n	-70.08 s		
	131		0.29 s	β^- , β^-n	-69.8 s	(9/2+)	
	132		0.12 s	β^- , β^-n	-~65 s		
	106		1.9 m	EC + β^+	-76.99 s	0^+	
	107		2.90 m	β^+ + EC	-78.40 s		
	108		10.5 m	EC	-81.90 s	0^+	
	109		18.0 m	β^+ , EC	-82.62 s	$7/2^+$	
	109		1.5 m?	?			
	110		4.1 h	EC	-85.834	0^+	
	111		35 m	EC 71%, β^+ 29%	-85.94	$7/2^+$	
	112		7.01%		-88.658	0^+	0.47_g 0.37_m
	113		115.1 d	EC	-88.332	$1/2^+$	
	113m		21 m	IT 91%, EC 9%	-88.253	$7/2^+$	
	114		0.67%		-90.560	0^+	
	115		0.38%		-90.035	$1/2^+$	$50_{s'}$
	116		14.8%		-91.526	0^+	$0.006_{m'}$
	117		7.75%		-90.399	$1/2^+$	$3_{s'}$
	117m		14.0 d	IT	-90.084	$11/2^-$	
	118		24.3%		-91.654	0^+	$0.08_{m'}$
	119		8.6%		-90.067	$1/2^+$	2
	119m		~250 d	IT	-89.977	$11/2^-$	
	120		32.4%		-91.102	0^+	0.16_g 0.001_m

TABLE OF NUCLIDES

Z	Nuclide El	A	Abundance or $t_{1/2}$	Decay Mode	Δ (MeV)	$J\pi$	$\sigma_n(b)$
50	Sn 121		27.1 h	β^- , no γ	-89.202	$3/2^+$	
	121m		55 y	β^-	-89.196	(11/2)-	
	122		4.56%		-89.946	0+	0.15_m
	123		129 d	β^-	-87.821	$11/2^-$	0.001_g
	123m		40.1 m	β^-	-87.796	(3/2)+	
	124		5.64%		-88.240	0+	0.13_m
	125		9.62 d	β^-	-85.903	$11/2^-$	
	125m		9.5 m	β^-	-85.876	$3/2^+$	
	126		$\approx 1 \times 10^5$ y	β^-	-86.024	0+	
	127		2.1 h	β^-	-83.79	(11/2-)	
	127m		4.1 m	β^-	-83.78	(3/2)+	
	128		59.3 m	β^-	-83.44	0+	
	129		2.2 m	β^-	-80.64	(3/2+)	
	129m		7.5 m	β^-	-80.60	(11/2-)	
	130		3.7 m	β^-	-80.38	0+	
	130m		1.7 m	β^-		(7-)	
	131		63 s	β^-	-77.48 s	(3/2+)	
	132		40 s	β^-	-76.60	0+	
	133		1.47 s	β^- , β^-n	-71.5		
	134		1.04 s	β^- , $\beta^-n \approx 17\%$		0+	
51	Sb 108		7.0 s	β^+	-72.40 s	(3+)	
	109		18.3 s	β^+ +EC	-76.12 s		
	110		23 s	$\beta^+ \approx 92\%$, EC $\approx 8\%$	-76.75	(3)+	
	111		75 s	β^+ , EC	-81.47	(5/2)+	
	112		54 s	β^+ , EC	-81.63	(3+)	
	113		6.7 m	EC, β^+	-84.443	(5/2)+	
	114		3.5 m	β^+ , EC	-84.14	(3)+	
	114		8 m	?			
	115		31.8 m	EC 67%, β^+ 33%	-87.005	$5/2^+$	
	116		16 m	EC 72%, β^+ 28%	-86.93	3+	
	116m		60.4 m	EC 81%, β^+ 19%	-86.32	8-	
	117		2.80 h	EC 97.5%, β^+ 2.5%	-88.654	$5/2^+$	
	118		3.5 m	EC, β^+	-87.967	1+	
	118		0.87 s	?			
	118m		5.00 h	EC 99.84%, β^+ 0.16%	-87.747	8-	
	119		38.0 n	EC	-89.483	$5/2^+$	
	120		15.8 m	EC 56%, β^+ 44%	-88.421	1+	
	120		5.76 d	EC		8-	
	121		57.3%		-89.588	$5/2^+$	6.1_g 0.06_m
	122		2.68 d	β^- 97.0%, EC 3.0%, β^+ 0.0063%	-88.323	2-	
	122m		4.2 m	IT	-88.160	(8-)	
	123		42.7%		-89.218	$7/2^+$	4.0_g 0.04_m
	124		60.20 d	β^-	-87.613	3-	7^{-s}
	124m ₁		93 s	IT 80%, β^- 20%	-87.603	(5)+	
	124m ₂		20.2 m	IT	-87.578		
	125		2.7 y	β^-	-88.252	$7/2^+$	
	126		12.4 d	β^-	-86.402	(8-)	
	126m		19.0 m	β^- 86%, IT 14%	-86.384	(5)+	
	127		3.9 d	β^-	-86.704	$7/2^+$	
	128(g)		9.1 h	β^-	-84.75	8-	
	128(m)		10.0 m	β^- 96.4%, IT 3.6%	-84.73	5+	
	129		4.4 h	β^-	-84.630	$7/2^+$	
	130		40 m	β^-	-82.38	(8-)	
	130		6.5 m	β^-		(4,5)+	
	131		23.03 m	β^-	-82.10 s	(7/2+)	
	132		2.8 m	β^-	-79.68	(4+)	
	132		4.2 m	β^-		(8-)	
	133		2.7 m	β^-	-78.98		
	134		10.4 s	β^- , β^-n 0.09%	-73.87 s		
	134		0.8 s	β^- , no γ	-73.87 s		
	135		1.70 s	β^- , β^-n 20%	-70.44 s	(7/2+)	
	136		0.82 s	β^- , β^-n 32%			
52	Te 107		2.1 s	α			

TABLE OF NUCLIDES

Z	Nuclide El	A	Abundance or $t_{1/2}$	Decay Mode	Δ (MeV)	$J\pi$	$\sigma_n(b)$
81	Tl	208	3.053 m	β^-	-16.768	(5+)	
		209	2.2 m	β^-	-13.650	(1/2+)	
		210	1.30 m	β^- , $\beta^-n \approx 0.007\%$	-9.251		
82	Pb	185	≈ 2 s	α	-11.74 s		
		186	8 s	$\alpha \approx 2.4\%$	-14.33 s	0+	
		187	17 s	$\alpha \approx 2.0\%$	-14.94 s		
		188	25 s	EC+ β^+ 97%, α 3%	-17.50 s	0+	
		189	51 s	EC+ β^+ 99+%, α 0.4%	-17.86 s		
		190	1.2 m	EC+ β^+ 99.8%, α 0.2%	-20.22 s	0+	
		191	1.3 m	EC+ β^+ 99+%, α 0.013%	-20.23 s		
		192	2.3 m	EC+ β^+ 99+%, α 0.007%	-22.29 s	0+	
		193	5.8 m	EC+ β^+	-22.07 s	(13/2+)	
		194	11 m	EC+ β^+	-23.81 s	0+	
		195	16.4 m	EC+ β^+	-23.55 s	(13/2+)	
		196	37 m	EC	-25.15 s	0+	
		197	?	EC+ β^+	-24.63 s	(3/2-)	
		197m	42 m	EC+ β^+ 81%, IT 19%	-24.31 s	(13/2+)	
		198	2.4 h	EC	-25.90 s	0+	
		199	1.5 h	EC $\approx 98.6\%$, $\beta^+ \approx 1.4\%$	-25.28	5/2-	
		199m	12.2 m	IT 93%, EC+ β^+ 7%	-24.86	13/2+	
		200	21.5 h	EC	-26.16 s	0+	
		201	9.4 h	EC 99+%, $\beta^+ \lesssim 0.034\%$	-25.327	5/2-	
		201m	61 s	IT	-24.699	13/2+	
		202	$\approx 3 \times 10^5$ y	EC, no γ	-25.942	0+	
		202m	3.62 h	IT 90.5%, EC 9.5%	-23.772	9-	
		203	52.0 h	EC	-24.794	5/2-	
		203m ₁	6.1 s	IT	-23.969	13/2+	
		203m ₂	0.48 s	IT	-21.844	29/2-	
		204	1.42%		-25.117	0+	0.7
		204m	66.9 m	IT	-22.932	9-	
		205	1.4×10^7 y	EC, no γ	-23.777	5/2-	3.8 ^{rs}
		206	24.1%		-23.795	0+	0.03 ₉
		207	22.1%		-22.463	1/2-	0.71 ₉
		207m	0.81 s	IT	-20.830	13/2+	
		208	52.3%		-21.759	0+	5.0×10^{-4}
		209	3.25 h	β^- , no γ	-17.624	9/2+	
		210	22.3 y	β^- 99+%, α $1.7 \times 10^{-6}\%$	-14.738	0+	0.5
		211	36.1 m	β^-	-10.492	(9/2)+	
		212	10.64 h	β^-	-7.562	0+	
		213	10.2 m	β^-	-3.14 s		
		214	26.8 m	β^-	-0.185	0+	
83	Bi	189	<1.5 s	α	-9.87 s		
		190	5.4 s	$\alpha \approx 90\%$	-10.85 s		
		191	13 s	$\alpha \approx 40\%$	-13.05 s		
		191m	≈ 20 s	α			
		192	42 s	$\alpha \approx 20\%$	-13.67 s		
		193	64 s	$\alpha \approx 60\%$	-15.56 s		
		193m	3.5 s	$\alpha \approx 25\%$			
		194	1.7 m	β^+ +EC 99+%, $\alpha < 0.2\%$	-15.98	(10-)	
		195	2.8 m	$\alpha < 0.2\%$	-17.68		
		195m	90 s	α 4%			
		196	4.5 m	β^+ +EC	-17.76 s		
		197(m)	8 m	β^+ +EC 99.89%, α 0.11%			
		198	11.8 m	EC+ β^+	-19.30 s	(7+)	
		198m	7.7 s	IT	-19.05 s	(10-)	
		199(g)	27 m	EC	-20.61 s	9/2-	
		199(m)	24.7 m	α	- ≈ 20.00 s		
		200	36 m	EC, β^+ (weak)	-20.46 s	7(+)	
		200m	0.40 s	IT	-20.03 s	10(-)	
		201	1.8 h	EC+ β^+	-21.41 s	9/2-	
		201m	59 m	EC+ β^+ , IT, $\alpha \gtrsim 0.02\%$	-20.56 s	(1/2+)	
		202	1.7 h	EC 99.5%, β^+ 0.5%	-21.04 s	5(+)	
		203	11.8 h	EC $\approx 99.7\%$, $\beta^+ \approx 0.3\%$	-21.60	9/2-	
		204	11.2 h	EC	-20.82 s	6+	
		205	15.3 d	EC 99.90%, β^+ 0.10%	-21.070	9/2-	
		206	6.243 d	EC, $\beta^+?$ $8 \times 10^{-4}\%$	-20.033	6+	
		207	38 y	EC 99+%, β^+ 0.012%	-20.058	9/2-	
		208	3.68×10^5 y	EC	-18.879	(5)+	

TABLE OF NUCLIDES

Z	Nuclide	Abundance or $t_{1/2}$	Decay Mode	$\Delta(\text{MeV})$	$J\pi$	$\sigma_n(b)$
El	A					
83	Bi 209	100%		-18.268	9/2-	0.019^{rs}_g 0.014^{rs}_m
	210	5.01 d	β^- 99+%, α $1.3 \times 10^{-4}\%$	-14.801	1-	0.050 sc
	210m	3.0×10^6 y	α	-14.530	9-	
	211	2.15 m	α 99.72%, β^- 0.28%	-11.865	(9/2)-	
	212	60.60 m	β^- 64.0%, β^- α 0.014%, α 36.0%	-8.135	1(-)	
	212m ₁	25 m	α \leq 93%, β^- \geq 7%	-7.88	[9-]	
	212m ₂	9 m	β^- \leq 100%		[15-]	
	213	45.6 m	β^- 97.8%, α 2.2%	-5.243	(9/2-)	
			β^- 99+%, β^- α 0.0031%, α 0.021%			
	214	19.7 m		-1.209	(1-)	
	215	7 m	β^-	1.71		
84	Po 193	\leq 1 s	α	-8.31 s		
	194	0.6 s	α	-10.81 s	0+	
	195(g)	4.5 s	α	-11.06 s		
	195(m)	2.0 s	α			
	196	5 s	α	-13.21 s	0+	
	197	58 s	α 90%	-13.23 s		
	197m	26 s	α			
	198	1.78 m	α 70%, EC + β^+ 30%	-15.07 s	0+	
	199	5.2 m	EC + β^+ 88%, α 12%	-15.05 s	(3/2-)	
	199m	4.2 m	EC + β^+ 61%, α 39%		(13/2+)	
	200	11.4 m	EC + β^+ 86%, α 14%	-16.74 s	0+	
	201	15.2 m	EC + β^+ 98.4%, α 1.6%	-16.41 s	3/2(-)	
	201m	8.9 m	IT 53%, EC + β^+ 44%, α 2.9%	-15.98 s	(13/2+)	
	202	44 m	EC + β^+ 98.0%, α 2.0%	-17.78 s	0+	
	203	33 m	EC + β^+ 99.89%, α 0.11%	-17.36	5/2-	
	203m	1.2 m	IT 96%, EC + β^+ 4%	-16.72	(13/2+)	
	204	3.57 h	EC 99.4%, α 0.6%	-18.25 s	0+	
	205	1.80 h	EC + β^+ 99.5%, α 0.5%	-17.576	5/2-	
	206	8.8 d	EC 94.5%, α 5.5%	-18.190	0+	
	207	5.7 h	EC 99.5%, β^+ 0.5%, α 0.008%	-17.150	5/2-	
	207m	2.8 s	IT	-15.766	19/2-	
	208	2.90 y	α 99+%, EC 0.0018%	-17.475	0+	
	209	102 y	α 99.74%, EC 0.26%	-16.373	1/2-	
	210	138.38 d	α	-15.963	0+	$<0.03^{rs}_g$ $<5 \times 10^{-4}^{rs}_m$ $<0.002_a$
	211	0.516 s	α	-12.444	(9/2+)	
	211m	25 s	α	-10.982	(25/2+)	
	212	0.30 μ s	α	-10.381	0+	
	212m	45 s	α	-7.476	[16+]	
	213	4 μ s	α	-6.663	9/2+	
	214	164 μ s	α	-4.479	0+	
	215	1.78 ms	α 99+%, β^- $2.3 \times 10^{-4}\%$	-0.540	(9/2)+	
	216	0.15 s	α	1.769	0+	
	217	<10 s	α	5.96 s		
	218	3.05 m	α 99+%, β^- 0.018%	8.355	0+	
85	At 196	0.3 s	α	-4.05 s		
	197	0.4 s	α	-6.03 s		
	198	4.9 s	α	-6.67		
	198m	1.5 s	α			
	199	7.2 s	α	-8.47		
	200(g)	42 s	α 53%, EC + β^+ 47%	-8.67 s		
	200(m)	4.3 s	α			
	201	1.5 m	α 71%, EC + β^+ 29%	-10.52 s		
	202	3.0 m	EC + β^+ 85%, α 15%	-10.52 s		
	203	7.3 m	EC + β^+ 69%, α 31%	-11.97 s		
	204	9.1 m	EC + β^+ 95.6%, α 4.4%	-11.97 s	(5+)	
	205	26 m	EC 87%, β^+ 3%, α 10%	-12.96 s	9/2-	
	206	31 m	EC 82%, β^+ 17%, α 1.0%	-12.73 s	(5+)	

NUCLEAR MODELS

At this point it is tempting to try to extend the ideas of the previous chapter to heavier nuclei. Unfortunately, we run into several fundamental difficulties when we do. One difficulty arises from the mathematics of solving the many-body problem. If we again assume an oversimplified form for the nuclear potential, such as a square well or an harmonic oscillator, we could in principle write down a set of coupled equations describing the mutual interactions of the A nucleons. These equations cannot be solved analytically, but instead must be attacked using numerical methods. A second difficulty has to do with the nature of the nuclear force itself. There is evidence to suggest that the nucleons interact not only through mutual two-body forces, but through three-body forces as well. That is, the force on nucleon 1 not only depends on the individual positions of nucleons 2 and 3, it contains an *additional* contribution that arises from the correlation of the positions of nucleons 2 and 3. Such forces have no classical analog.

In principle it is possible to do additional scattering experiments in the three-body system to try (in analogy with the two-body studies described in Chapter 4) to extract some parameters that describe the three-body forces. However, we quickly reach a point at which such a microscopic approach obscures, rather than illuminates, the essential physics of the nucleus. It is somewhat like trying to obtain a microscopic description of the properties of a gas by studying the interactions of its atoms and then trying to solve the dynamical equations that describe the interatomic forces. Most of the physical insight into the properties of a gas comes from a few general parameters such as pressure and temperature, rather than from a detailed microscopic theory.

We therefore adopt the following approach for nuclei. We choose a deliberately oversimplified theory, but one that is mathematically tractable and rich in physical insight. If that theory is fairly successful in accounting for at least a few nuclear properties, we can then improve it by adding additional terms. Through such operations we construct a *nuclear model*, a simplified view of nuclear structure that still contains the essentials of nuclear physics. A successful model must satisfy two criteria: (1) it must reasonably well account for previously measured nuclear properties, and (2) it must predict additional properties that can be measured in new experiments. This system of modeling complex processes is a common one in many areas of science; biochemists model the complex processes such as occur in the replication of genes, and atmospheric

scientists model the complex dynamics of air and water currents that affect climate.

5.1 THE SHELL MODEL

Atomic theory based on the shell model has provided remarkable clarification of the complicated details of atomic structure. Nuclear physicists therefore attempted to use a similar theory to attack the problem of nuclear structure, in the hope of similar success in clarifying the properties of nuclei. In the atomic shell model, we fill the shells with electrons in order of increasing energy, consistent with the requirement of the Pauli principle. When we do so, we obtain an inert core of filled shells and some number of valence electrons; the model then assumes that atomic properties are determined primarily by the valence electrons. When we compare some measured properties of atomic systems with the predictions of the model, we find remarkable agreement. In particular, we see regular and smooth variations of atomic properties *within* a subshell, but rather sudden and dramatic changes in the properties when we fill one subshell and enter the next. Figure 5.1 shows the effects of a change in subshell on the ionic radius and ionization energy of the elements.

When we try to carry this model over to the nuclear realm, we immediately encounter several objections. In the atomic case, the potential is supplied by the Coulomb field of the nucleus; the subshells ("orbits") are established by an external agent. We can solve the Schrödinger equation for this potential and calculate the energies of the subshells into which electrons can then be placed. In the nucleus, there is no such external agent; the nucleons move in a potential that they themselves create.

Another appealing aspect of atomic shell theory is the existence of spatial orbits. It is often very useful to describe atomic properties in terms of spatial orbits of the electrons. The electrons can move in those orbits relatively free of collisions with other electrons. Nucleons have a relatively large diameter compared with the size of the nucleus. How can we regard the nucleons as moving in well defined orbits when a single nucleon can make many collisions during each orbit?

First let's examine the experimental evidence that supports the existence of nuclear shells. Figure 5.2 shows measured proton and neutron separation energies, plotted as deviations from the predictions of the semiempirical mass formula, Equation 3.28. (The gross changes in nuclear binding are removed by plotting the data in this form, allowing the shell effects to become more apparent.) The similarity with Figure 5.1 is striking—the separation energy, like the atomic ionization energy, increases gradually with N or Z except for a few sharp drops that occur at the same neutron and proton numbers. We are led to guess that the sharp discontinuities in the separation energy correspond (as in the atomic case) to the filling of major shells. Figure 5.3 shows some additional evidence from a variety of experiments; the sudden and discontinuous behavior occurs at the same proton or neutron numbers as in the case of the separation energies. These so-called "magic numbers" (Z or $N = 2, 8, 20, 28, 50, 82$, and 126) represent the effects of filled major shells, and any successful theory must be able to account for the existence of shell closures at those occupation numbers.

118 BASIC NUCLEAR STRUCTURE

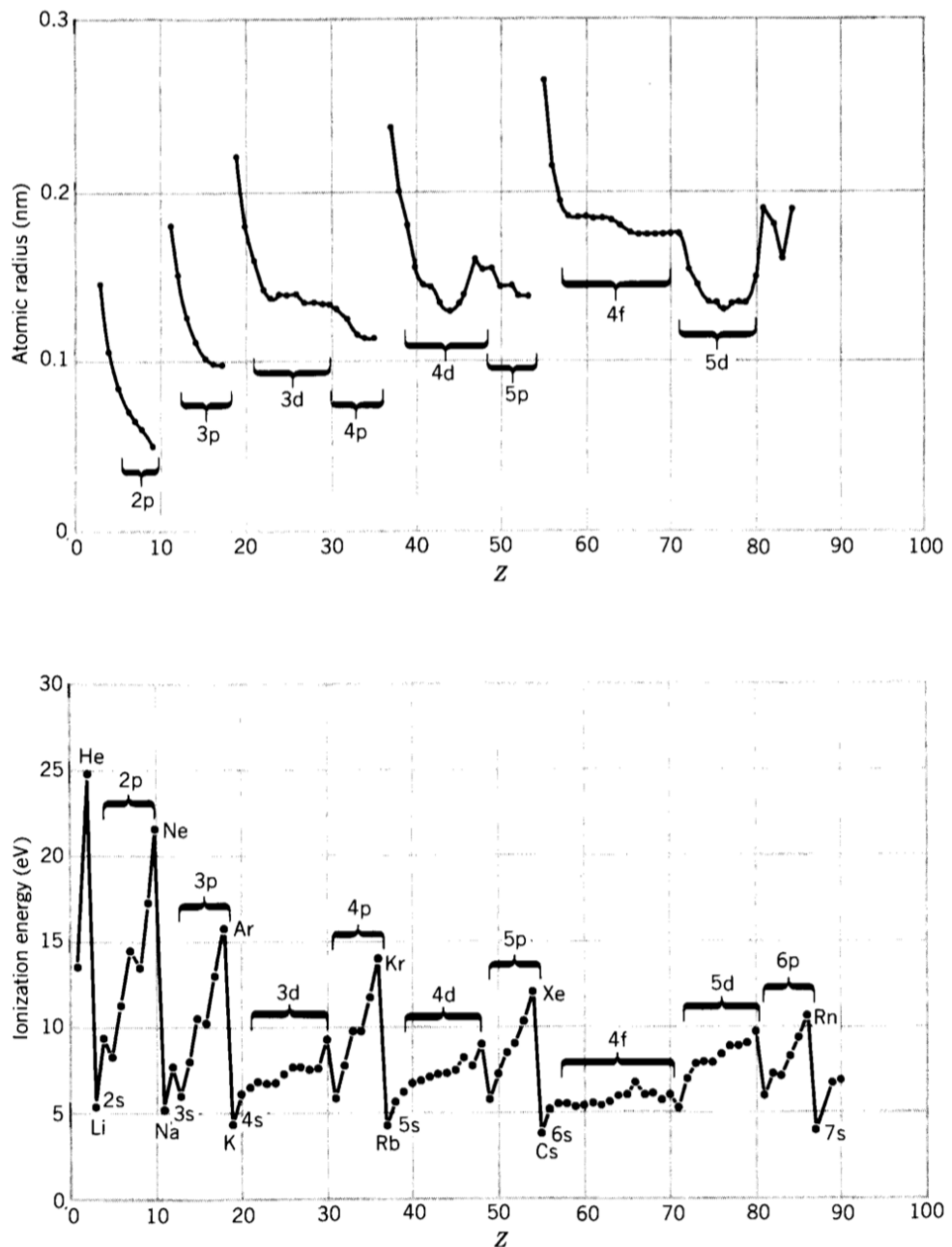


Figure 5.1 Atomic radius (top) and ionization energy (bottom) of the elements. The smooth variations in these properties correspond to the gradual filling of an atomic shell, and the sudden jumps show transitions to the next shell.

The question of the existence of a nuclear potential is dealt with by the fundamental assumption of the shell model: the motion of a single nucleon is governed by a potential caused by all of the other nucleons. If we treat each individual nucleon in this way, then we can allow the nucleons in turn to occupy the energy levels of a series of subshells.

The existence of definite spatial orbits depends on the Pauli principle. Consider in a heavy nucleus a collision between two nucleons in a state near the very

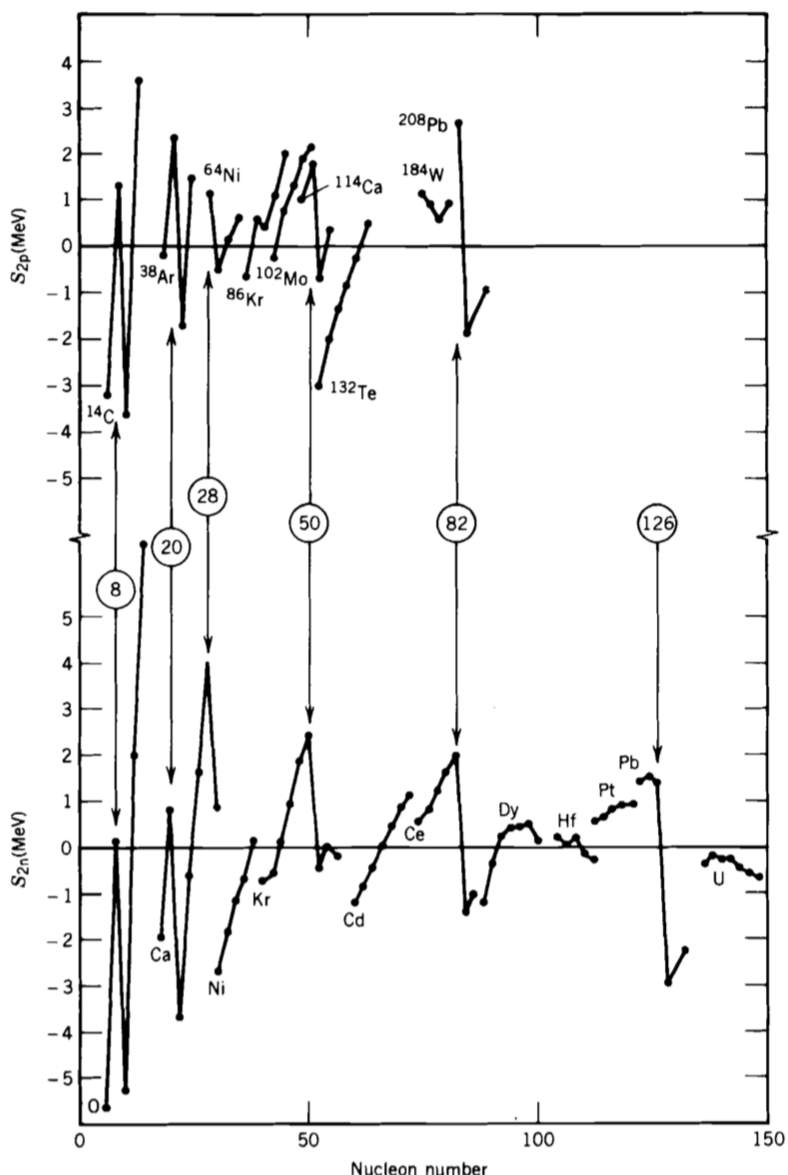


Figure 5.2 (Top) Two-proton separation energies of sequences of isotones (constant N). The lowest Z member of each sequence is noted. (Bottom) Two-neutron separation energies of sequences of isotopes. The sudden changes at the indicated “magic numbers” are apparent. The data plotted are differences between the measured values and the predictions of the semiempirical mass formula. Measured values are from the 1977 atomic mass tables (A. H. Wapstra and K. Bos, *Atomic Data and Nuclear Data Tables* **19**, 215 (1977)).

bottom of the potential well. When the nucleons collide they will transfer energy to one another, but if all of the energy levels are filled up to the level of the valence nucleons, there is no way for one of the nucleons to gain energy except to move up to the valence level. The other levels near the original level are filled and cannot accept an additional nucleon. Such a transfer, from a low-lying level to the valence band, requires more energy than the nucleons are likely to transfer in

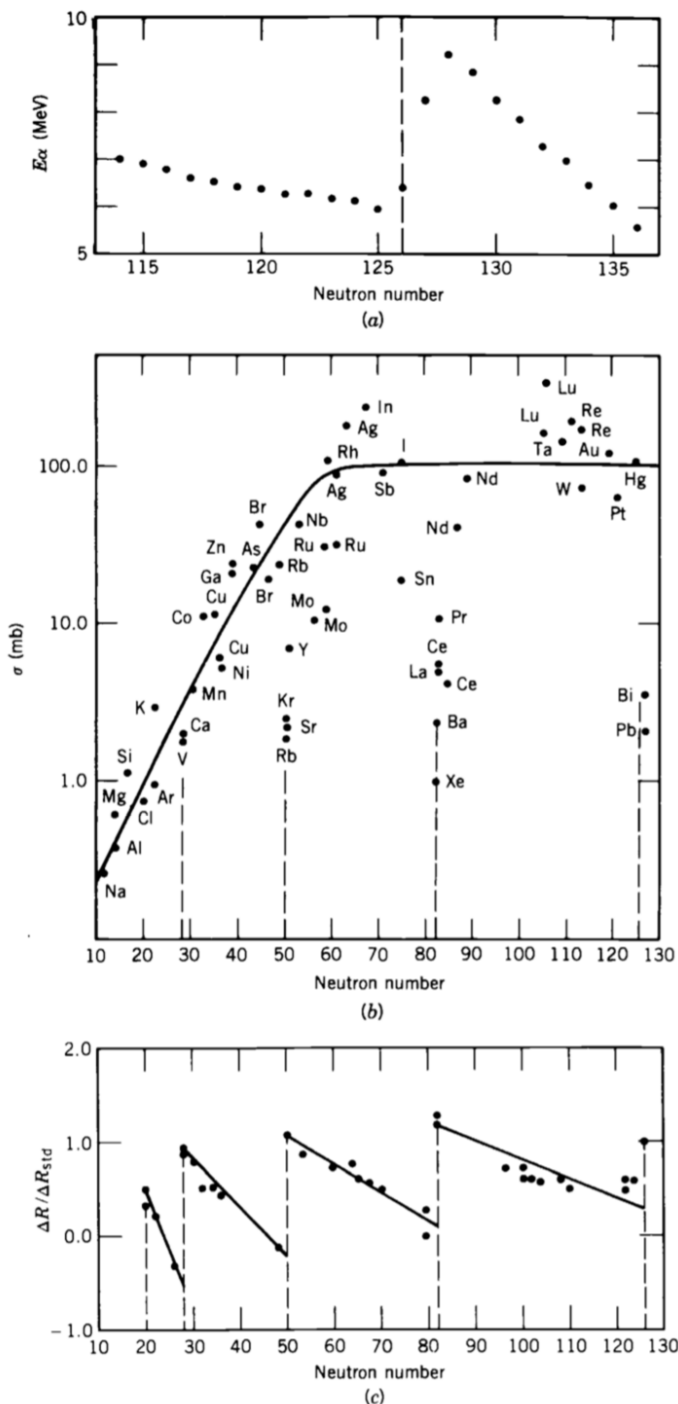


Figure 5.3 Additional evidence for nuclear shell structure. (a) Energies of α particles emitted by isotopes of Rn. Note the sudden increase when the daughter has $N = 126$ (i.e., when the parent has $N = 128$). If the daughter nucleus is more tightly bound, the α decay is able to carry away more energy. (b) Neutron-capture cross sections of various nuclei. Note the decreases by roughly two orders of magnitude near $N = 50$, 82 , and 126 . (c) Change in the nuclear charge radius when $\Delta N = 2$. Note the sudden jumps at 20 , 28 , 50 , 82 , and 126 and compare with Figure 5.1. To emphasize the shell effects, the radius difference ΔR has been divided by the standard ΔR expected from the $A^{1/3}$ dependence. From E. B. Shera et al., *Phys. Rev. C* **14**, 731 (1976).

a collision. Thus the collisions cannot occur, and the nucleons can indeed orbit as if they were transparent to one another!

Shell Model Potential

The first step in developing the shell model is the choice of the potential, and we begin by considering two potentials for which we solved the three-dimensional Schrödinger equation in Chapter 2: the infinite well and the harmonic oscillator. The energy levels we obtained are shown in Figure 5.4. As in the case of atomic physics, the degeneracy of each level is the the number of nucleons that can be put in each level, namely $2(2\ell+1)$. The factor of $(2\ell+1)$ arises from the m_ℓ degeneracy, and the additional factor of 2 comes from the m_s degeneracy. As in atomic physics, we use spectroscopic notation to label the levels, with one important exception: the index n is *not* the principal quantum number, but simply counts the number of levels with that ℓ value. Thus 1d means the first (lowest) d state, 2d means the second, and so on. (In atomic spectroscopic notation, there are no 1d or 2d states.) Figure 5.4 also shows the occupation

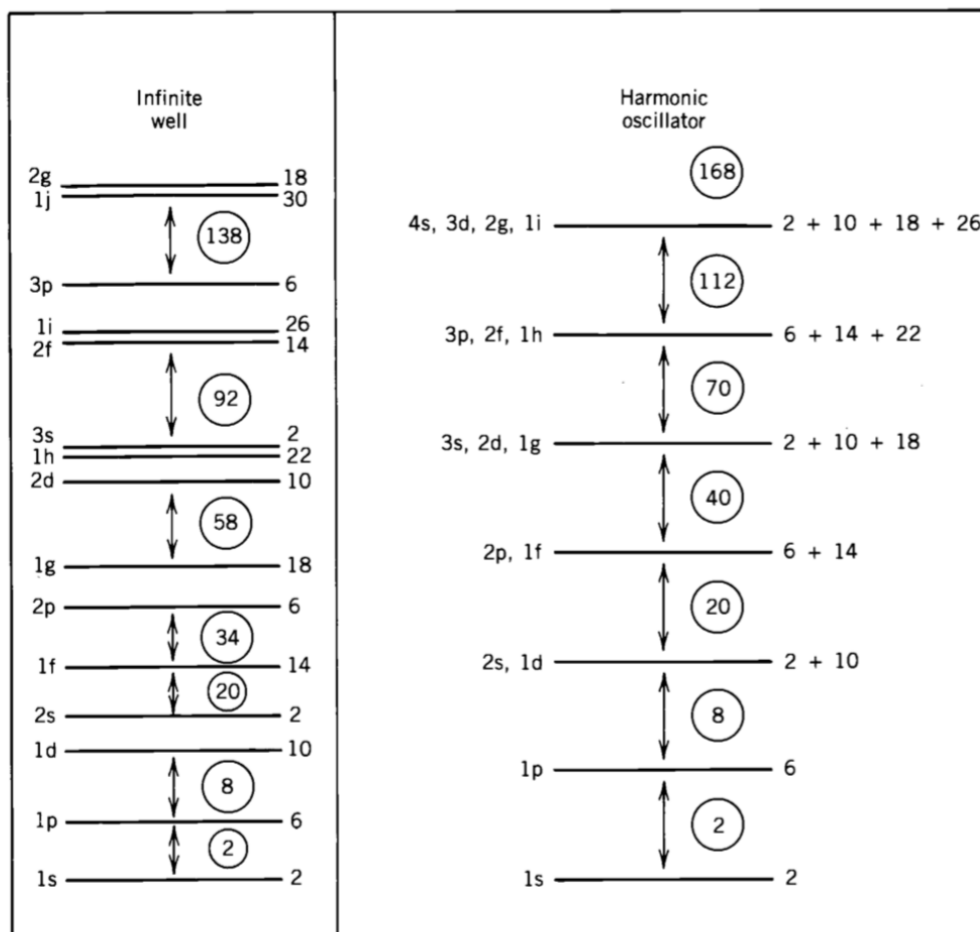


Figure 5.4 Shell structure obtained with infinite well and harmonic oscillator potentials. The capacity of each level is indicated to its right. Large gaps occur between the levels, which we associate with closed shells. The circled numbers indicate the total number of nucleons at each shell closure.

12

NEUTRON PHYSICS

As the uncharged member of the nucleon pair, the neutron plays a fundamental role in the study of nuclear forces. Unaffected by the Coulomb barrier, neutrons of even very low energy (eV or less) can penetrate the nucleus and initiate nuclear reactions. In contrast, part of our lack of understanding of processes in the interior of stars results from the difficulty of studying proton-induced reactions at energies as low as keV. On the other hand, the lack of Coulomb interaction presents some experimental problems when using neutrons as a nuclear probe: energy selection and focusing of an incident neutron beam are difficult, and neutrons do not produce primary ionization events in detectors (neutrons passing through matter have negligible interactions with the atomic electrons).

The first experimental observation of the neutron occurred in 1930, when Bothe and Becker bombarded beryllium with α particles (from radioactive decay) and obtained a very penetrating but nonionizing radiation, which they assumed to be a high-energy γ ray. Soon thereafter, Curie and Joliot noticed that when this radiation fell on paraffin, an energetic proton was emitted. From the range of these protons, they determined their energy to be 5.3 MeV. If the radiation under study were indeed γ 's, protons could be knocked loose from paraffin by a Compton-like collision; from the Compton-scattering formula, they computed that the energy of this “ γ radiation” would be at least 52 MeV to release such protons. An emitted γ of such an energy seemed extremely unlikely. In 1932, Chadwick provided the correct explanation, identifying the unknown radiation as a neutral (therefore penetrating and nonionizing) particle with a mass nearly the same as that of the proton. Thus in a head-on collision, a 5.3-MeV neutron could transfer its energy entirely to the struck proton. Chadwick did additional recoil experiments with neutrons and confirmed his hypothesis, and he is generally credited with being the discoverer of the neutron.

The free neutron is unstable against β decay, with a half-life of 10.6 min. In nuclei, the bound neutron may be much longer-lived (even stable) or much shorter-lived. Despite the instability of free neutrons, their properties are measured to high precision, particularly the magnetic dipole moment, $\mu = -1.91304184 \pm 0.00000088 \mu_N$, and the neutron-proton mass difference, $m_n - m_p = 1.29340 \pm 0.00003$ MeV.

Basic research with neutrons goes back almost to the earliest days of nuclear physics, and it continues to be a vital and exciting research field today. For example, interference effects with neutron beams have permitted some basic

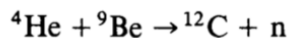
aspects of quantum mechanics to be demonstrated for the first time. The *electric* dipole moment of the neutron should vanish if the neutron were an elementary particle or even a composite particle in which the binding forces were symmetric with respect to the parity and time-reversal operations. Many careful and detailed experiments have been done, and all indicate a vanishing electric dipole moment, but the limit has been pushed so low ($10^{-25} \text{ e} \cdot \text{cm}$) that it is almost possible to distinguish among certain competing theories for the interactions among the elementary particles. The so-called Grand Unified Theories that attempt to unify the strong (nuclear), electromagnetic, and weak (β -decay) interactions predict that the conservation of nucleon number (actually baryon number) can break down, and that a neutron could convert into its antiparticle, the antineutron, and then back again to a neutron. No evidence has yet been seen for this effect either, but current research is trying to improve the limits on our knowledge of the neutron-antineutron conversion frequency.

12.1 NEUTRON SOURCES

Beams of neutrons can be produced from a variety of nuclear reactions. We cannot accelerate neutrons as we can charged particles, but we can start with high-energy neutrons and reduce their energy through collisions with atoms of various materials. This process of slowing is called "moderating" the neutrons. The resulting neutrons can have very low energies, which by convention are given the following designations:

Thermal	$E \approx 0.025 \text{ eV}$
Epithermal	$E \sim 1 \text{ eV}$
Slow	$E \sim 1 \text{ keV}$
Fast	$E = 100 \text{ keV}-10 \text{ MeV}$

α -Beryllium Sources The reaction responsible for the discovery of the neutron can be used to produce a source of neutrons suitable for use in the laboratory. The stable isotope of beryllium, ^9Be , has a relatively loosely bound neutron (1.7 MeV binding energy). If a typical α particle from a radioactive decay (5–6 MeV) strikes a ^9Be nucleus, a neutron can be released:



The Q value for this reaction is 5.7 MeV. If we mix together a long-lived α -emitting material, such as ^{226}Ra , and ${}^9\text{Be}$, there will be a constant rate of neutron production. From ^{226}Ra and its daughters there are α 's emitted with energies from about 5 to nearly 8 MeV, and thus we find neutrons with an energy spectrum up to 13 MeV. The neutrons are not monoenergetic because of (1) the many α groups, (2) the slowing of α 's that will occur by collision in any solid material, (3) the various directions of emission that can occur for the neutrons relative to the α 's (whose direction we do not know), and (4) the possibility that ${}^{12}\text{C}$ is left in an excited state. The most probable neutron energy is about 5 MeV, and the neutron production rate is about 10^7 neutrons per second for each Ci of ^{226}Ra . A typical neutron spectrum is shown in Figure 12.1.

Because of the high γ emission of ^{226}Ra and its daughters, the radium-beryllium neutron source has largely been replaced with sources using ^{210}Po (138 d),

446 NUCLEAR REACTIONS

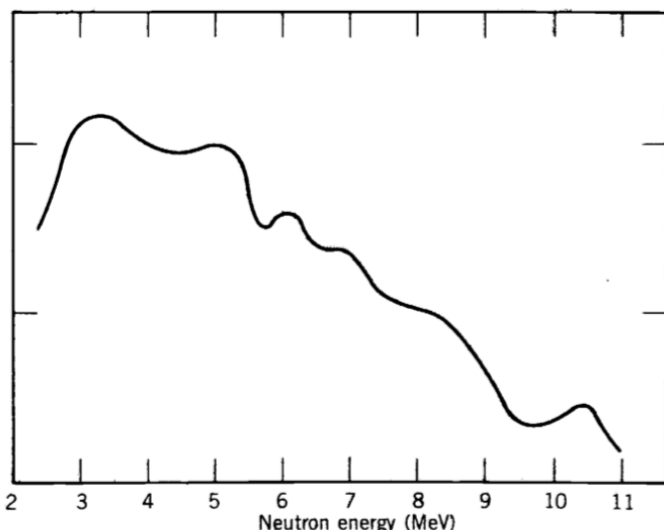


Figure 12.1 Neutron energy spectrum from a Ra-Be source, measured with a proton recoil counter. Several neutron groups are present; they result from reactions induced by α 's with differing energies and in which the ^{12}C is left either in the ground state or the 4.43- or 7.6-MeV excited states.

^{238}Pu (86 y), and ^{241}Am (458 y). These sources produce about $2\text{--}3 \times 10^6$ neutrons per second per Ci of α activity.

Photoneutron Sources In a process similar to the (α, n) sources discussed above, we can use the (γ, n) reaction to produce neutrons. The advantage of photoneutron production is that we can make the neutrons more nearly monoenergetic, particularly if the photon source is nearly monoenergetic. For example, ^{24}Na emits a γ of 2.76 MeV, absorption of which would be sufficient to overcome the neutron binding energy of ^9Be :



The yield is acceptable (2×10^6 neutrons/s per Ci of ^{24}Na), but the half-life is short (15 h). The neutron energy is about 0.8 MeV. A longer-lived isotope ^{124}Sb (60 d) emits a strong γ whose energy just exceeds the ^9Be neutron binding energy; the emitted neutron has a much lower energy, about 24 keV.

Spontaneous Fission A common source of neutrons is the spontaneous fission of isotopes such as ^{252}Cf (2.65 y). Neutrons are produced directly in the fission process, at a rate of about 4 per fission. The fission occurs in only about 3% of the decays (α decay accounts for the rest), and the neutron production rate is 2.3×10^{12} neutrons/s per gram of ^{252}Cf or 4.3×10^9 n/s per Ci of ^{252}Cf . The neutron energies are characteristic of fission—a continuous distribution with an average energy of 1–3 MeV.

Nuclear Reactions There are of course many nuclear reactions that produce neutrons. These require an accelerator to produce a beam of particles to initiate the reaction, and thus they are not as convenient as the radioactive-decay type of sources discussed previously. However, by carefully selecting the incident energy and the angle at which we observe the emitted neutron, we can obtain a

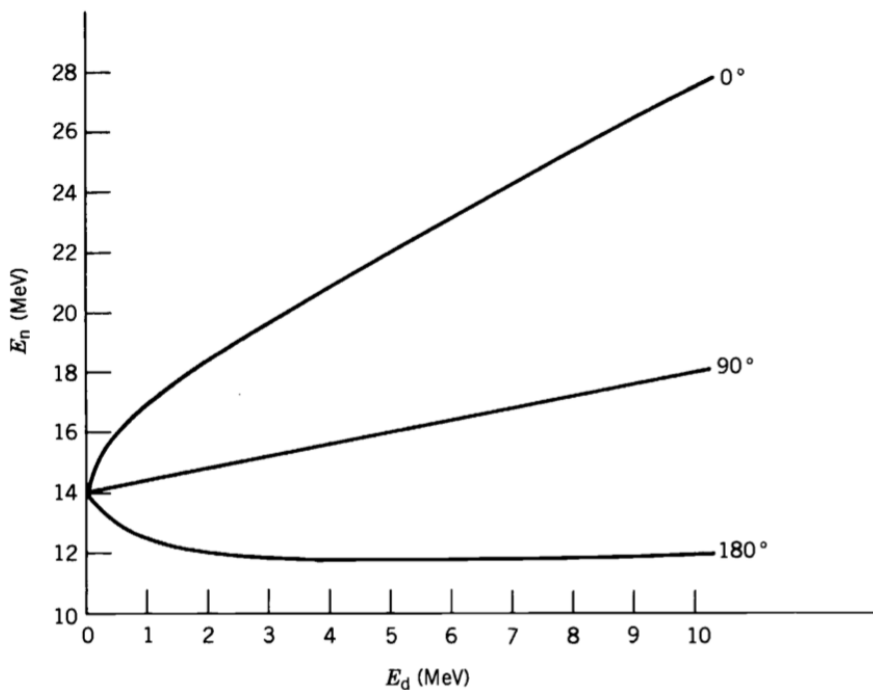


Figure 12.2 Neutrons emitted in the ${}^3\text{H}(\text{d}, \text{n}){}^4\text{He}$ reaction.

reasonably monoenergetic beam of almost any desired energy. Some reactions that might be used are

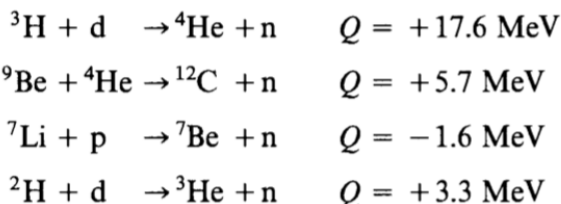


Figure 12.2 illustrates the dependence of the neutron energy in the first of these reactions on the incident energy and on the direction of the outgoing neutron.

Reactor Sources The neutron flux near the core of a nuclear fission reactor can be quite high—typically 10^{14} neutrons/cm²/s. The energy spectrum extends to 5–7 MeV but peaks at 1–2 MeV. These neutrons are generally reduced to thermal energies within the reactor, but there are also fast neutrons present in the core. Cutting a small hole in the shielding of the reactor vessel permits a beam of neutrons to be extracted into the laboratory for experiments. The high neutron fluxes from a reactor are particularly useful for production of radioisotopes by neutron capture, as in neutron activation analysis.

12.2 ABSORPTION AND MODERATION OF NEUTRONS

As a beam of neutrons travels through bulk matter, the intensity will decrease as neutrons are removed from the beam by nuclear reactions. For fast neutrons, many reactions such as (n, p) , (n, α) , or $(\text{n}, 2\text{n})$ are possible, but for slow or thermal neutrons the primary cause of their disappearance is capture, in the form

448 NUCLEAR REACTIONS

of the (n, γ) reaction. Often the cross sections for these capture reactions are dominated by one or more resonances, where the cross section becomes very large. Off resonance, the cross section decreases with increasing velocity like v^{-1} ; thus as the neutrons slow down (become moderated) due to elastic and inelastic scattering processes, absorption becomes more probable. Neutrons with initial energy in the 1-MeV range would undergo many scattering processes until their energies were reduced to the eV range, where they would have a high probability of resonant or nonresonant absorption.

In crossing a thickness dx of material, the neutrons will encounter $n dx$ atoms per unit surface area of the beam or the material, where n is the number of atoms per unit volume of the material. If σ_t is the total cross section (including scattering processes, which will tend to divert neutrons from the beam), then the loss in intensity I is

$$dI = -I\sigma_t n dx \quad (12.1)$$

and the intensity decreases with absorber thickness according to an exponential relationship:

$$I = I_0 e^{-\sigma_t n x} \quad (12.2)$$

Keep in mind that this expression refers only to monoenergetic neutrons—the original intensity of neutrons of a certain energy decreases according to Equation 12.2. Of course, we may at the same time be creating neutrons of lower energy (by scattering, for example), which may have a very different cross section, but this effect is not included in Equation 12.2. We therefore cannot use it reliably to calculate the decrease in the *total number* of neutrons, only the change in intensity of those with a given initial energy.

Let's consider an elastic collision between a neutron of initial energy E and velocity v with a target atom of mass A initially at rest. Elementary application of the laws of conservation of energy and linear momentum gives the ratio between the final neutron energy E' and the initial energy:

$$\frac{E'}{E} = \frac{A^2 + 1 + 2A \cos \theta}{(A + 1)^2} \quad (12.3)$$

where θ is the scattering angle in the center-of-mass system (but E and E' are measured in the laboratory system). For no scattering ($\theta = 0$), Equation 12.3 gives $E'/E = 1$, as it should. The maximum energy loss occurs for a head-on collision ($\theta = 180^\circ$):

$$\left(\frac{E'}{E}\right)_{\min} = \left(\frac{A - 1}{A + 1}\right)^2 \quad (12.4)$$

Notice that for $A = 1$ (scattering from hydrogen), the neutron gives all its energy to the struck proton.

For neutron energies of about 10 MeV and below, the scattering is mostly s wave and thus (in the center-of-mass system) largely independent of θ . The values of E'/E are uniformly distributed between $E'/E = 1$ and the minimum value given by Equation 12.4, as shown in Figure 12.3a.

Because each neutron will scatter many times, we must repeatedly calculate the energy loss. In the case of the second scattering, the incident neutrons are no

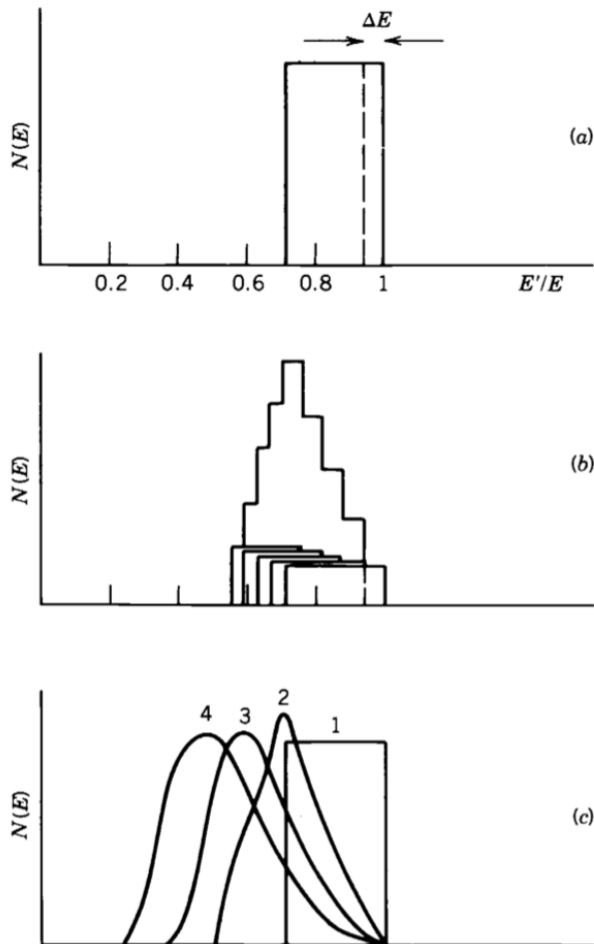


Figure 12.3 (a) A monoenergetic neutron of energy E gives, after a single s-wave scattering from ^{12}C , a flat distribution of laboratory energies E' from $0.72E$ to E . (b) Dividing the scattered distribution into five narrow, nearly monoenergetic distributions of width ΔE , we get after a second scattering the five flat distributions shown, whose sum is the peaked distribution. (c) An exact calculation of the energy distribution after 1, 2, 3, and 4 scatterings.

longer monoenergetic but rather are distributed as in Figure 12.3a. We can approximate this effect by considering each interval of width ΔE to be a new generation of approximately monoenergetic neutrons giving the result shown in Figure 12.3b. Continuing this process, we obtain the succeeding “generations” of energy distributions shown in Figure 12.3c.

To make the calculations more quantitative, we define the parameter ξ to represent the average value of $\log(E/E')$ after a single collision:

$$\xi = \left[\log \frac{E}{E'} \right]_{\text{av}} \quad (12.5)$$

$$= \frac{\int \log \left[\frac{(A+1)^2}{A^2 + 1 + 2A \cos \theta} \right] d\Omega}{\int d\Omega} \quad (12.6)$$

450 NUCLEAR REACTIONS

Table 12.1 Moderating Properties of Various Nuclei

Nucleus	ξ	n (for thermalization)
^1H	1.00	18
^2H	0.725	25
^4He	0.425	43
^{12}C	0.158	110
^{238}U	0.0084	2200

where $d\Omega$ is the element of solid angle in the center-of-mass system. Here again we assume the scattering to be isotropic. Carrying out the integration gives

$$\xi = 1 + \frac{(A - 1)^2}{2A} \log \frac{A - 1}{A + 1} \quad (12.7)$$

The average value of $\log E'$ is decreased after each collision by an amount ξ , and after n collisions, the average value of $\log E'$ is $\log E'_n$:

$$\log E'_n = \log E - n\xi \quad (12.8)$$

which follows directly from Equation 12.5.

Table 12.1 shows values of ξ for some commonly used moderators. If our goal is to reduce the average neutron energy from that which is typical for neutrons emitted in fission ($E \sim 2$ MeV) to that which is characteristic of thermal motion ($E'_n \sim 0.025$ eV), the number of generations of collisions is shown in Table 12.1.

The previous calculation has assumed the atoms from which the neutrons scatter to be at rest. This is certainly a good approximation for MeV neutrons, but as thermal energies are approached, we find the thermal motion of the atoms of the moderator to be comparable to the speeds of the neutrons. The scattering in this case is better analyzed using statistical mechanics, and we can simply assume that after a sufficient time the neutrons will reach thermal equilibrium with the moderator at a temperature T . In this case, the neutrons are described by a Maxwellian speed distribution:

$$f(v) dv = 4\pi n \left(\frac{m}{2\pi kT} \right)^{3/2} v^2 e^{-mv^2/2kT} dv \quad (12.9)$$

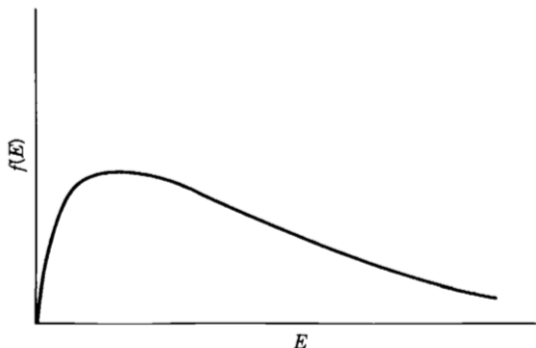


Figure 12.4 Maxwellian energy distribution, a representation of the neutron energy spectrum after many scatterings.

where $f(v) dv$ gives the fraction of neutrons with speeds between v and $v + dv$. Here m is the neutron mass and n is the total number of neutrons per unit volume. Rewriting this in terms of energy gives

$$f(E) dE = \frac{2\pi n}{(\pi kT)^{3/2}} E^{1/2} e^{-E/kT} dE \quad (12.10)$$

which is illustrated in Figure 12.4 and looks similar to Figure 12.3c, showing the thermalizing effect of even a few generations of collisions.

12.3 NEUTRON DETECTORS

Because neutrons produce no direct ionization events, neutron detectors must be based on detecting the secondary events produced by nuclear reactions, such as (n, p) , (n, α) , (n, γ) , or $(n, \text{fission})$, or by nuclear scattering from light charged particles, which are then detected.

For slow and thermal neutrons, detectors based on the (n, p) and (n, α) reactions provide a direct means for observing neutrons from the signal left by the energetic p or α resulting from the reaction. The isotope ^{10}B is commonly used, by producing an ionization chamber or a proportional counter filled with BF_3 gas or lined with boron metal or a boron compound. The reaction is



where the ${}^7\text{Li}$ is preferentially left in an excited state with energy 0.48 MeV. (Natural boron consists of about 20% of the isotope ^{10}B , so materials enriched in ^{10}B increase the efficiency of the detector.) For thermal neutrons, the cross section is about 3840 b, a very large value, and the cross section follows the $1/v$ law up to about 100 keV, so the dependence of cross section on incident energy is featureless (no resonances are present) and predictable (Figure 12.5).

There is also another advantage of the $1/v$ dependence of the cross section. Suppose we are observing a collimated beam of neutrons or an isotropic flux (perhaps near the core of a reactor) that has a velocity distribution of $n(v) dv$ neutrons per unit volume with speeds between v and $v + dv$. The flux passing through the detector will be $n(v)v dv$, and if the counter contains N boron nuclei each with cross section σ , the probability per second of an interaction (or counting rate, if we are able to detect and count every interaction) is

$$dR = N\sigma n(v)v dv \quad (12.11)$$

for neutrons of speeds between v and $v + dv$. For neutrons of all speeds, the total counting rate is

$$R = \int N\sigma n(v)v dv \quad (12.12)$$

$$= NC \int n(v) dv \quad (12.13)$$

where the last step assumes that $\sigma \propto v^{-1}$, so that the product σv is the constant C . The integral then gives the total number of neutrons per unit volume n , and

B. CROSS SECTIONS

Definitions, Units, and Examples. We now turn to a more quantitative consideration of reaction probabilities. The probability of a nuclear process is generally expressed in terms of a cross section σ that has the dimensions of an area. This originates from the simple picture that the probability for the reaction between a nucleus and an impinging particle is proportional to the cross-sectional target area presented by the nucleus. Although this classical picture does not hold for reactions with charged particles that have to overcome Coulomb barriers or for slow neutrons (it does hold fairly well for the total probability of a fast neutron interacting with a nucleus), the cross section is a useful measure of the probability for any nuclear reaction. For a beam of particles striking a thin target, that is, a target in which the beam is attenuated only infinitesimally, the cross section for a particular process is defined by the equation

$$R_i = I n x \sigma_i, \quad (4-3)$$

where R_i is the number of processes of the type under consideration occurring in the target per unit time,

I is the number of incident particles per unit time,

n is the number of target nuclei per cubic centimeter of target,

σ_i is the cross section for the specified process, expressed in square centimeters, and

x is the target thickness in centimeters.

The target thickness is often given in terms of weight per unit area, which can be readily converted to nx , the number of target nuclei per square centimeter.

The total cross section for collision with a fast particle is never greater than twice⁶ the geometrical cross-sectional area of the nucleus, and therefore fast-particle cross sections are rarely much larger than 10^{-24} cm^2 (radii of the heaviest nuclei are about 10^{-12} cm). Hence a cross section of 10^{-24} cm^2 is considered "as big as a barn," and 10^{-24} cm^2 has been named the **barn**, a unit generally used in expressing cross sections and often abbreviated b. The millibarn (mb, 10^{-3} b), microbarn (μb , 10^{-6} b), and nanobarn (nb, 10^{-9} b) are also commonly used.

As an example of the application of (4-3), consider a 1-h bombardment of a foil of metallic manganese, 10 mg/cm^2 thick, in a $1-\mu\text{A}$ beam of 35-MeV α particles. If the cross section of the $(\alpha, 2n)$ reaction on ^{55}Mn at this energy is 200 mb and if energy degradation of the beam in traversing the target can be neglected, how many ^{57}Co nuclei ($t_{1/2} = 270 \text{ d}$) will be formed? First remember

⁶The reason why total cross sections may be as large as $2\pi R^2$ is briefly mentioned in footnote 12 on p. 31.

that $1 \text{ A} = 6.2 \times 10^{18}$ electronic charges per second so that $1 \mu\text{A}$ of (doubly charged) α particles is 3.1×10^{12} α particles per second. The number of $(\alpha, 2n)$ reactions is, from (4-3), $3.1 \times 10^{12} \times (0.01/55) \times 6.02 \times 10^{23} \times 200 \times 10^{-27} = 6.8 \times 10^7$. Neglecting decay during the 1-h irradiation, we get for the number of ^{57}Co nuclei formed $3600 \times 6.8 \times 10^7 = 2.4 \times 10^{11}$. The ^{57}Co disintegration rate at the end of the irradiation, from $dN/dt = \lambda N$, would be $[0.693/(270 \times 24 \times 60)] \times 2.4 \times 10^{11} = 4.3 \times 10^5 \text{ min}^{-1}$.

Equation 4-3 applies when there is a well-defined beam of particles incident on a target. Another important situation concerns a sample embedded in a uniform flux of particles incident on it from all directions. This is what happens, for example, in a nuclear reactor. It can be shown that, for a sample containing N nuclei in a flux of ϕ particles per square centimeter per second, the rate of reactions of type i , which have a cross section σ_i , is given by

$$R_i = \phi N \sigma_i. \quad (4-4)$$

This applies, regardless of the shape of the sample, provided that the particle flux is not appreciably attenuated by sample absorption anywhere in the sample.

As an example, we calculate how long a 60-mg piece of Co wire has to be placed in a flux of 5×10^{13} thermal neutrons per square centimeter per second to make 1 mCi (1 millicurie = $3.7 \times 10^7 \text{ dis s}^{-1}$; see chapter 1, section B) of $5.27\text{-y } ^{60}\text{Co}$. The cross section for the reaction $^{59}\text{Co}(n, \gamma) ^{60}\text{Co}$ is 37 b. From (4-4) we have

$$R = 5 \times 10^{13} \times \frac{0.060}{59} \times 6.02 \times 10^{23} \times 37 \times 10^{-24} = 1.13 \times 10^{12} \text{ atoms s}^{-1}.$$

From $dN/dt = \lambda N$ we find that 1 mCi of ^{60}Co corresponds to 8.87×10^{15} atoms.

Thus it will take $8.87 \times 10^{15}/1.13 \times 10^{12} = 7.85 \times 10^3 \text{ s}$, or approximately 2.2 h, to produce 1 mCi of ^{60}Co .

Beam Attenuation Measurements. If instead of a thin target we consider a thick target, that is, one in which the intensity of the incident particle beam is attenuated, the attenuation $-dI$ in the infinitesimal thickness dx is given by the equation

$$-dI = In\sigma_i dx,$$

where σ_i is the total cross section for removal of the incident particles from the beam. Integration gives

$$I = I_0 e^{-n\sigma_i x}. \quad (4-5)$$

Just what processes are included in σ_i depends considerably on the particular experimental arrangement, especially on the energy selectivity of the detector used to measure the transmitted beam and on the solid angle it

subtends. Thus for example, the cross section for small-angle elastic scattering may or may not be included in σ_t .

Beam attenuation measurements, of course, measure always the effect of the entire target substance, whether it is a single nuclide, an isotopic mixture, or even a compound.

Partial Cross Sections. As we emphasized in the preceding paragraph, beam attenuation or transmission experiments can be used only to determine total interaction cross sections, and (4-5) is not applicable to cross sections for specific reactions that constitute only part of the total interaction. Yet it is usually cross sections for particular processes on elementary, or even isotopically pure, substances that are of interest, such as the (n, p) reaction on ^{35}Cl or the $(\alpha, 3n)$ reaction on ^{65}Cu . Thin-target experiments are then needed so that (4-3) or (4-4) is applicable. The requirements for target thickness are particularly stringent if the cross section of interest varies rapidly with bombarding energy, as is the case for most medium-energy charged-particle reactions; the target then must be thin enough to avoid not only intensity attenuation but also appreciable energy degradation.

Sometimes the angular distribution of particles resulting from a particular process is of interest. In this case it is convenient to define a differential cross section $d\sigma/d\Omega$; this is the cross section for that part of the process in which the particles are emitted into unit solid angle at a particular angle Ω . Then the cross section for the overall process under consideration is $\sigma = \int (d\sigma/d\Omega) d\Omega$.

Elastic Scattering. The simplest consequence of a nuclear collision is so-called elastic scattering; this is a process that can occur at all energies and with all particles and that is not properly a reaction at all. An event is termed an elastic scattering if the particles do not change their identity during the process and if the sum of their kinetic energies (ignoring molecular and atomic excitations and bremsstrahlung) remains constant. Elastic scattering of charged particles with energies below the Coulomb barrier of the target nucleus is the Rutherford scattering described in chapter 2. As the energy of the bombarding particle is increased, the particle may penetrate the Coulomb barrier to the surface of the target nucleus, and the elastic scattering will then also have a contribution from the nuclear forces. For neutrons, of course, elastic scattering is caused by nuclear forces at all energies.

Elastic scattering may generally be considered to arise from the optical-model potential discussed in section D. With neutrons of very low energies there is also a significant contribution from so-called compound elastic scattering, since the compound nucleus formed by the amalgamation of such a neutron with the target nucleus (see section D) has a small but finite probability of emitting a neutron with all its original energy. For all other particles compound elastic scattering is negligible.

We designate the cross section for all events other than (potential) elastic scattering as the *reaction cross section*. Compound elastic scattering is formally included in the reaction cross section, although it cannot be distinguished experimentally from other elastic scattering.

Maximum Reaction Cross Sections for Neutrons. It might be expected that a nucleus that interacts with everything that hits it would have a reaction cross section of πR^2 , where R is the sum of the radii of the interacting particles. As we see, this is correct at high energies only, because the wave nature of the incident particle causes the upper limit of the reaction cross section to be

$$\sigma_r = \pi (R + \lambda)^2,$$

where λ is the reduced de Broglie wavelength ($\lambda/2\pi$) of the incident particle in the center-of-mass system and may be obtained from $\lambda = \hbar/p$. Here p is the *relative momentum* of the two particles computed from (C-6) in appendix C.

Although cross section limits are properly derived by quantum-mechanical methods (see, e.g., B1, chapter 8), we give a semiclassical treatment that shows the essence of the problem and points up the important role played by angular-momentum considerations. We first treat reactions with incident neutrons and then proceed to discuss the additional effects of Coulomb repulsion.

Angular Momentum in Nuclear Reactions. A collision between a neutron and a target nucleus may be characterized classically by what would be the distance of closest approach of the two particles if there were no interaction between them. This distance b , usually called the **impact parameter**, is shown in figure 4-1. The angular momentum of the system is normal to the relative momentum p and of magnitude

$$L = pb. \quad (4-6)$$

The de Broglie relation between momentum and wavelength of a particle

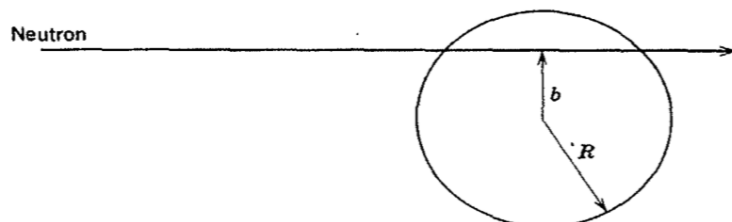


Fig. 4-1 Collision with impact parameter b between a neutron and target nucleus with interaction radius R .

allows (4-6) to be rewritten as

$$L = \frac{\hbar b}{\lambda}. \quad (4-7)$$

Note that the entire treatment is in the center-of-mass system and that λ is thus the reduced wavelength in that system. See appendix C for transformations between laboratory and center-of-mass systems.

As b may evidently assume any value between 0 and R , the relative angular momentum will vary continuously between 0 and $\hbar R/\lambda$. We know, though, that this is not acceptable; quantum mechanics requires that the component of angular momentum in a particular direction be an integer when expressed in units of \hbar :

$$L = l\hbar, \quad \text{where } l = 0, 1, 2, \dots \quad (4-8)$$

Combination of (4-7) and (4-8) gives

$$b = l\lambda. \quad (4-9)$$

Equation 4-9 is not to be interpreted as meaning that only certain values of b are possible; such control over b would violate the uncertainty principle. Rather it means that a range of values of b corresponds to the same value of the angular momentum. In particular,

$$l\lambda < b < (l+1)\lambda \quad (4-10)$$

corresponds to an angular momentum of $l\hbar$. This interpretation is illustrated in figure 4-2. From this figure it can be seen that the cross-sectional area that corresponds to a collision with angular momentum $l\hbar$ is

$$\begin{aligned} \sigma_l &= \pi\lambda^2[(l+1)^2 - l^2] \\ &= \pi\lambda^2(2l+1). \end{aligned} \quad (4-11)$$

If it is assumed that each particle hitting the nucleus causes a reaction, then

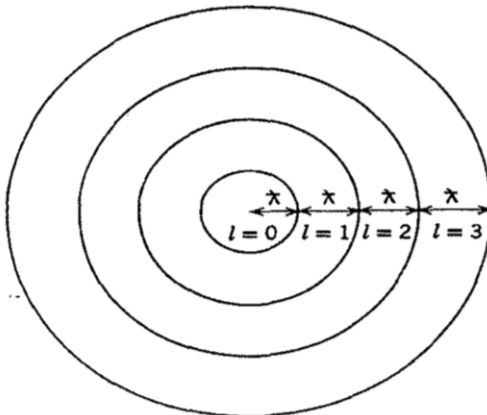


Fig. 4-2 The incident beam is perpendicular to the plane of the figure. The particles with a particular l are considered to strike within the designated ring.

(4-11) gives the partial cross section for a nuclear reaction characterized by angular momentum $l\hbar$, and the reaction cross section may be obtained by summing (4-11) over all values of l from 0 to the maximum l_m :

$$\sigma_r = \pi\chi^2 \sum_0^{l_m} (2l + 1). \quad (4-12)$$

The summation in (4-12) may be easily evaluated if it is recalled that the sum of the first N integers is equal to $[N(N + 1)]/2$. The expression for the reaction cross section becomes

$$\sigma_r = \pi\chi^2 (l_m + 1)^2. \quad (4-13)$$

The maximum value of l may be estimated from (4-9) by limiting the maximum impact parameter to the interaction radius R :

$$l_m = \frac{R}{\chi}. \quad (4-14)$$

Substitution of (4-14) into (4-13) yields the result already given on p. 118 for the maximum possible reaction cross section:

$$\sigma_r = \pi (R + \chi)^2. \quad (4-15)$$

This result suggests the possibility of nuclear-reaction cross sections that are several orders of magnitude larger than the geometrical cross section of the nucleus, a possibility that is realized in slow-neutron reactions. The largest thermal-neutron cross section known is that of ^{135}Xe , $2.65 \times 10^6 \text{ b}$. (See also section E.)

In the quantum-mechanical treatment of the problem (B1) the result for the total reaction cross section is not (4-12), but

$$\sigma_r = \pi\chi^2 \sum_{l=0}^{\infty} (2l + 1)T_l, \quad (4-16)$$

where T_l is defined as the **transmission coefficient** for the reaction of a neutron with angular momentum l and may have values between zero and one; it represents the fraction of incident particles with angular momentum l that penetrate within the range of nuclear forces. Our semiclassical treatment assigns unity to T_l for all values of l up to and including l_m , as defined in (4-14); for all higher values of l , the transmission coefficients are zero. The role of angular momentum here is analogous to the one that it plays in β and γ emission, discussed in chapter 3. It should be mentioned here that the semiclassical result is quite right for $R/\chi < 1$, where the only contribution comes from $l = 0$ and the reaction cross section has $\pi\chi^2$ as its upper limit.

Centrifugal Barrier. Expression 4-14 for the maximum l value can be reinterpreted to mean that a particle that approaches a nucleus with relative angular momentum l must have a reduced de Broglie wavelength

$\lambda \leq R/l$. Since $\epsilon = p^2/2\mu = \hbar^2/2\mu\lambda^2$, where ϵ is the relative kinetic energy, p the relative momentum, and μ the reduced mass of the system, we have the condition

$$\epsilon \geq \frac{l^2\hbar^2}{2\mu R^2}, \quad (4-17)$$

where R may be taken as the sum of the radii of projectile particle and target nucleus. Condition 4-17 implies that, quite apart from any Coulomb barrier, there is for particles of angular momentum l an additional barrier, called the centrifugal barrier. In the quantum-mechanical treatment of the problem l^2 is replaced by $l(l+1)$, so that the proper expression for the centrifugal barrier or centrifugal potential is

$$V_l = \frac{l(l+1)\hbar^2}{2\mu R^2}. \quad (4-18)$$

Reaction Cross Sections with Charged Particles. The effect of the Coulomb repulsion on a reaction cross section may be easily estimated within the spirit of the semiclassical analysis. The Coulomb repulsion will bring the relative kinetic energy of the system from ϵ when the particles are very far apart to $\epsilon - V_c$ when the two particles are just touching, where V_c is the Coulomb barrier:

$$V_c = \frac{Z_a Z_A e^2}{R}, \quad (4-19)$$

and where Z_a and Z_A are the atomic numbers of incident particle and target nucleus, respectively. Further, the deflection of the particles causes the maximum impact parameter that leads to a reaction to be less than R , as illustrated in figure 4-3. From this figure it is seen that the trajectory of the particle is tangential to the nuclear surface when it approaches with the maximum impact parameter b_m and that the relative momentum at the

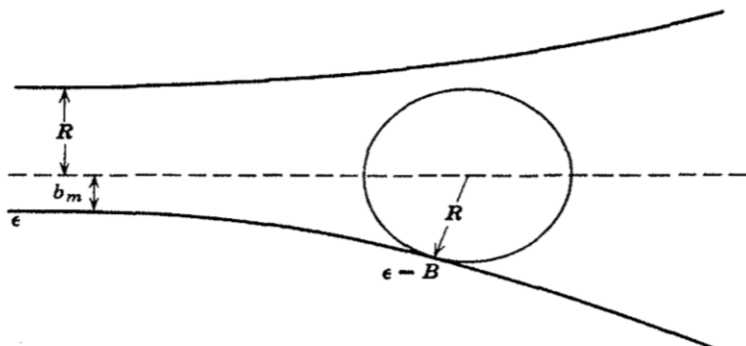


Fig. 4-3 Classical trajectories for charged particles with impact parameters R and b_m .

The mean free path may also be immediately expressed in terms of the density of nucleons within the nucleus and the effective average cross section $\bar{\sigma}$ for the interaction of the incident particle with the nucleons within the nucleus:

$$\Lambda = \frac{1}{\rho \bar{\sigma}}, \quad (4-31)$$

which establishes a relationship between optical-model parameters and the effective nucleon-nucleon interaction cross section within the nucleus.

Summary. Before leaving the subject of the optical model we review what it can and cannot do. It can be used to calculate, via the quantity η_l ,

1. The cross section for elastic scattering by (4-25).
2. The total-reaction cross section by (4-26).
3. The angular distribution for elastic scattering by (4-28).

The optical model can give no information about the relative probabilities of the various reactions that may occur after the incident particle has been absorbed in the nucleus, nor can it account for the very pronounced resonances seen in slow-neutron reactions.

2. Compound-Nucleus Model

The first model for nuclear reactions that enjoyed much success in the detailed interpretation of experimental data was the compound-nucleus model introduced by Bohr (B3) in 1936.

Basic Ideas. In the compound-nucleus model it is assumed that the incident particle, upon entering the target nucleus, amalgamates with it in such a way that its kinetic energy (which has been increased by the depth of the potential well on entering the nucleus) is distributed randomly among all the nucleons. The resulting nucleus, which is in an excited quasi-stationary state, is called the compound nucleus. The state is said to be quasi-stationary because its excitation energy makes it unstable with respect to the emission of particles, although its lifetime is thought to be long (typically 10^{-14} – 10^{-19} s) compared to the time for a nucleon to traverse the nucleus (10^{-20} – 10^{-23} s). The nucleons in the compound nucleus presumably exchange energy with each other through many collisions, and the finite lifetime comes about because it is possible for a statistical fluctuation in the energy distribution to concentrate enough energy on a nucleon (or a cluster of nucleons) to allow it to escape. The most probable fluctuations are those that concentrate only a part of the excitation energy on the escaping particle, and so we expect that its kinetic energy will be less than

the maximum possible and that the residual nucleus will still be in an excited state. Thus if the original excitation energy of the compound nucleus is great enough, there may be the sequential emission of several particles from the excited compound nucleus, each with a relatively low kinetic energy. The similarity of this model to that for the escape of molecules from a drop of hot liquid has caused the emission of particles from excited nuclei to be called "evaporation."

In the compound-nucleus model, then, a nuclear reaction is divided into two distinct and independent steps:

1. Capture of the incident particle with a random sharing of the energy among the nucleons in the compound nucleus.
2. The evaporation of particles from the excited compound nucleus.

The independence of the two steps is one of the central features of the model. It means that, if a compound nucleus can be produced in more than one way, its subsequent decay into reaction products should be quite independent of its mode of formation.

The excitation energy U of the compound nucleus is given by

$$U = \frac{M_A}{M_A + M_a} T_a + S_a, \quad (4-32)$$

where M_A and M_a are the atomic masses of the target and bombarding particles, respectively; T_a is the laboratory kinetic energy of the bombarding particle; and S_a is the binding energy of particle a in the compound nucleus.

Because beams of bombarding particles generally have a finite energy spread, the "quasi-stationary state" of the compound nucleus includes, in fact, many excited states. Lack of detailed knowledge about this composite of states causes most of the difficulties in the analysis of the compound-nucleus model. This problem, however, is not serious for thermal neutrons because only a single excited state is involved.

Slow-Neutron Reactions. Since the excitation energy of a compound nucleus formed by capture of a slow neutron is only slightly higher than the binding energy of the neutron in the compound nucleus, a very long time would be required before enough energy would, through a fluctuation, be concentrated on a neutron again to allow it to escape from the potential well. The probability for de-excitation by γ emission is therefore much higher, and the main reaction with slow neutrons is the (n, γ) reaction.

A typical excitation function for a slow-neutron reaction, that with silver as a target, is shown in figure 4-9 for the energy range from 0.01 to 100 eV. Three important characteristics of such slow-neutron excitation functions can be seen in figure 4-9:

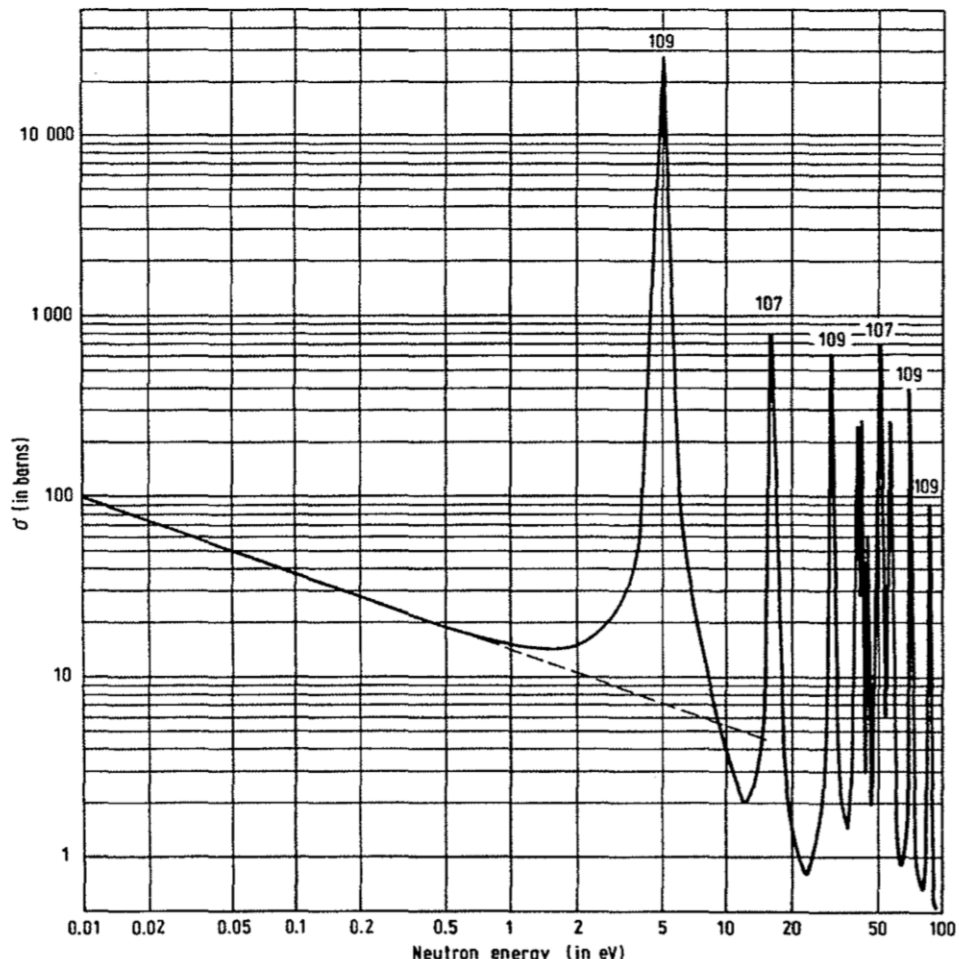


Fig. 4-9 Neutron cross section of silver as a function of energy in the region from 0.01 to 100 eV. The data as plotted are for silver of normal isotopic composition; however, each resonance peak has been assigned to one of the two silver isotopes, as indicated by mass number for a few of the peaks. (Data from reference N2.)

1. The cross sections show enormous fluctuations over a very small energy range, that is, resonances are apparent.
2. The widths of the resonances are small (~ 0.1 eV).
3. The spacing between the resonances is large compared to their widths; the spacings vary from the order of keV in the lightest elements to the order of eV for the heaviest).

The small widths of the resonances lead to the conclusion, by use of the

Heisenberg uncertainty principle, that the compound nucleus has a lifetime of about 10^{-14} – 10^{-15} s, which is long compared to the transit time of a thermal neutron across a medium-weight nucleus, $\sim 10^{-18}$ s. This conclusion suggested the idea of the quasi-stationary state for the compound nucleus. Further, the observation that the average spacing between the resonances is 100 to 1000 times smaller than the average spacing between single-particle levels showed that the quasi-stationary excited state of the compound nucleus must involve the excitation of many particles. For these reasons the optical model is not directly applicable to slow-neutron reactions; however, it is possible to make a connection between optical-model parameters and cross sections *averaged over many resonances* (F2).

Independence Hypothesis in the Resonance Region. Although the (n, γ) reaction is by far the most likely process with low-energy neutrons, it is not the only possible one. In some light elements, where Coulomb barriers are low, (n, p) or (n, α) reactions may compete with (n, γ) if binding energies of these charged particles are sufficiently low. For the heaviest elements fission is often the most probable process. In these reactions resonances are again observed in the excitation functions.

Since the compound-nucleus model divides the reaction into two parts—formation and decay of the compound nucleus—the relative probabilities of the various possible events should be completely determined by the quantum state of the compound nucleus. In particular, if the resonances do not overlap, the behavior of the compound nucleus is essentially governed by the properties of a single quantum state (the resonant state) and should thus be independent of the manner in which the state was formed. This means, for example, that the relative amount of γ -ray emission and neutron emission will be the same when nucleus 2X is irradiated with neutrons and ^{z-1}X is irradiated with protons as long as the energies of the particles are such that they form the same nonoverlapping resonant state. This conclusion is known as the “independence hypothesis.” We return to it again in the more ambiguous situation of overlapping states.

Breit-Wigner Formula. The rapidly varying cross section illustrated in figure 4-9 shows that the amplitudes η_i of the outgoing waves (see p. 130) are very sensitive functions of the energy in this low-energy region. In the first solution of this problem by G. Breit and E. Wigner,¹⁰ the quantities η_i were not directly calculated; rather, perturbation theory was used to solve the problem in the two steps suggested by Bohr involving the formation and decay of the compound nucleus. It is useful to give the results of their calculations for a general reaction:



¹⁰ See reference R1 for a complete discussion of theory and experiment with slow neutrons.

an element Z has an energy rather close to but slightly greater than the K absorption edge of some element of slightly lower Z and is strongly absorbed by that element but not by the next higher one. These two neighboring elements will thus have very different absorption coefficients for the particular rays, and the one that absorbs more strongly is called the critical absorber for these X rays. Critical absorption can also be applied to L -emission lines, especially of heavy elements.

As an example, consider the K_{α} X rays of zinc ($Z = 30$) which have an energy of 8.6 keV. The K absorption edges of ^{29}Cu and ^{28}Ni are 9.0 and 8.3 keV, respectively. Therefore, nickel is a good absorber for zinc K_{α} X rays, and copper is not (figure 6-14). The K_{α} X rays of gallium ($Z = 31$), on the other hand, are strongly absorbed both in nickel and copper because their energy is 9.2 keV, but they are not absorbed well in zinc whose K absorption edge is 9.7 keV.

Critical absorbers can be used to advantage, for example, to suppress one X-ray line so that the spectrum of a neighboring one can be measured cleanly. Both the X-ray emission lines and the absorption edges of the elements can be found in tables (L2). An example of the use of critical absorption is discussed in chapter 11, section B,5.

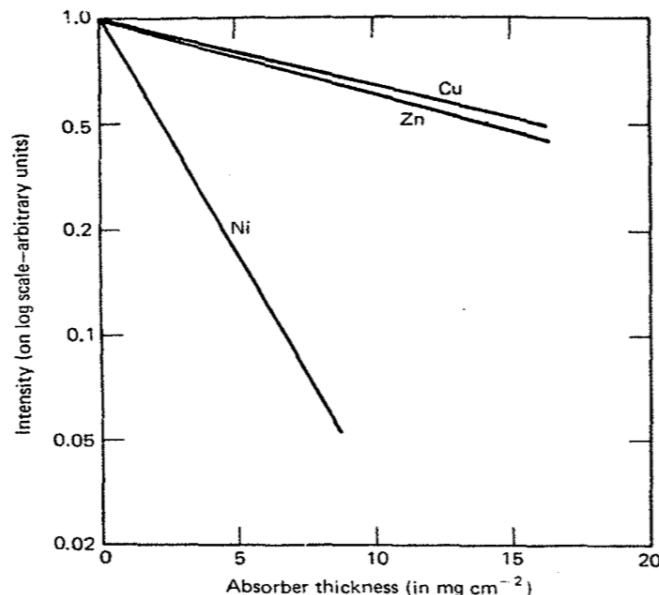


Fig. 6-14 Absorption of zinc K_{α} X rays in zinc, copper, and nickel. (These absorption curves were calculated from data given in reference C1.)

D. NEUTRONS

Because neutrons carry no charge, their interaction with electrons is exceedingly small, and primary ionization by neutrons is a completely negligible effect. The interaction of neutrons with matter is confined to nuclear effects, which include elastic and inelastic scattering and nuclear reactions such as (n, γ) , (n, p) , (n, α) , $(n, 2n)$, and fission. These nuclear interactions have been discussed in chapter 4; how they are applied to detection and measurement of neutrons is discussed in chapter 7, section E.

Slowing Down of Neutrons. From the description of nuclear reactions given in chapter 4, section E, it will be recalled that thermal neutrons, neutrons whose energy distribution is approximately that of gas molecules at ordinary temperatures, are very efficient at producing nuclear reactions. Because of this fact processes for reducing the energy of high-energy neutrons produced in nuclear reactions to a thermal energy distribution have received much theoretical and experimental study.

Fast neutrons may lose large amounts of energy in inelastic collisions, especially with heavy nuclei. This process ceases to be effective after intermediate energies are reached and does not produce slow neutrons. Most slowing down is accomplished through a process of many successive elastic collisions with nuclei. Because of the conservation of momentum a neutron of energy E_0 making an elastic collision with a heavy nucleus bounces off with most of its original energy, giving up no more energy than $4AE_0/(A + 1)^2$ to the recoil nucleus, where A is the mass number of the target nucleus. The lighter the nucleus with which a neutron collides, the greater the fraction of the neutron's kinetic energy that can be transferred in the elastic collision. For this reason hydrogen-containing substances such as paraffin or water are the most effective slowing-down media for neutrons.

In the elastic scattering of neutrons with energies below about 10 MeV all energy transfers between zero and the upper limit, $4AE_0/(A + 1)^2$, are equally probable. Thus the probability that a neutron of energy E_0 has a residual energy between E and $E + dE$ is

$$P(E) dE = \frac{dE}{4AE_0/(A + 1)^2},$$

and the average energy retained by the neutron is

$$\begin{aligned} \bar{E} &= \int_{E_0(1-4A/(A+1)^2)}^{E_0} P(E)E dE = \frac{(A+1)^2}{4AE_0} \int_{E_0(1-4A/(A+1)^2)}^{E_0} E dE \\ &= E_0 \left[1 - \frac{2A}{(A+1)^2} \right]. \end{aligned} \quad (6-31)$$

From this result it is seen that the average value of E/E_0 is independent of E_0 ; therefore the average value of E/E_0 after n collisions is simply

$$\overline{\frac{E_n}{E_0}} = \left[1 - \frac{2A}{(A+1)^2} \right]^n. \quad (6-32)$$

The average value after n collisions is a rather misleading quantity, as the distribution of energies is strongly skewed. The probability that a neutron of initial energy E_0 has an energy between E_n and $E_n + dE_n$ after n elastic collisions with hydrogen nuclei may be obtained from the recursion relation⁸

$$P_n(E_n) dE_n = \int_{E_n}^{E_0} [dE_{n-1} P_{n-1}(E_{n-1})] \left[\frac{dE_n}{E_{n-1}} \right], \quad (6-33)$$

where the first bracketed term is the probability of obtaining energy between E_{n-1} and $E_{n-1} + dE_{n-1}$ in $n-1$ collisions, and the second bracketed term is the probability of going from the interval $E_{n-1} \rightarrow E_{n-1} + dE_{n-1}$ to the interval $E_n \rightarrow E_n + dE_n$ in the n th collision. The integration is performed over the variable E_{n-1} . Equation 6-33 has the solution (ignoring thermal motion):

$$P_n(E_n) = \frac{1}{(n-1)! E_0} \left(\ln \frac{E_0}{E_n} \right)^{n-1}. \quad (6-34)$$

Another question of interest is the average number of collisions required to slow a neutron of energy E_0 down to an energy E . We may write for the energy after n collisions

$$E = E_0 f_1 f_2 \cdots f_i \cdots f_n, \quad (6-35)$$

where

$$f_i = \frac{E_i}{E_{i-1}}. \quad (6-36)$$

As we stated before, f_i has equal probability for all values between 1 and $1 - 4A/(A+1)^2$. It is clear that (6-35) has an infinite number of possible solutions for any value of n above a certain minimum value determined by the mass of the scattering nucleus. It is tempting to estimate the average value of n by putting the average value of f from (6-32) into (6-35), but this would be wrong. It would be wrong for the same reason that the average square of a set of random numbers is, in general, not equal to the square of the average. The solution to the problem, however, can be immediately obtained by a simple transformation of (6-35), which turns the problem into a more familiar one whose answer is well known.

Take the logarithm of both sides of (6-35):

$$\ln \left(\frac{E}{E_0} \right) = \ln (f_1 f_2 \cdots f_i \cdots f_n) = \sum_{i=1}^n \ln f_i;$$

define $x_i = -\ln f_i$ so that

$$\ln \left(\frac{E_0}{E} \right) = \sum_{i=1}^n x_i. \quad (6-37)$$

⁸ The recursion relations for heavier nuclei are more complicated than (6-33), since it is not possible for neutrons of all values of E_{n-1} to go to E_n in a single collision.

Again, an infinite number of values of n will satisfy (6-37), but now the average value of n is equivalent to the average number of collision-free segments (the number of collisions + 1) traversed by a gas molecule when it travels a "distance" $\ln(E_0/E)$. The answer to this problem is well known; the average number of collisions is just the distance traveled divided by the mean-free path.⁹ The number of collision-free segments is then

$$\bar{n} = \frac{\ln(E_0/E)}{\bar{x}} + 1 = \frac{\ln(E_0/E)}{\ln(\bar{E}_{i-1}/\bar{E}_i)} + 1, \quad (6-38)$$

where the quantities with bars over them denote mean values. The mean value of $\ln(\bar{E}_{i-1}/\bar{E}_i)$ may be obtained in the same manner as \bar{E} in (6-31) [cf. (9-6)]; the result is

$$\overline{\ln\left(\frac{E_{i-1}}{E_i}\right)} = 1 - \frac{(A-1)^2}{2A} \ln\left(\frac{A+1}{A-1}\right). \quad (6-39)$$

Substituting (6-39) into (6-38) gives

$$\bar{n} = \frac{\ln(E_0/E)}{1 - [(A-1)^2/2A] \ln[(A+1)/(A-1)]} + 1. \quad (6-40)$$

Equation 6-40 just derived gives the average number of collisions required to slow a neutron of energy E_0 down to an energy E . For collisions with protons ($A = 1$) the denominator in (6-40) becomes unity, hence $E_n = E_0 e^{1-\bar{n}}$; approximately 20 collisions are therefore necessary to reduce neutrons from a few million electron volts to thermal energies (about 0.04 eV at ordinary room temperature). Paraffin about 20 cm thick surrounding a neutron source is adequate for reducing most neutrons to the thermal energy distribution. The whole slowing-down process requires less than 10^{-3} s.

The probable eventual fate of a thermal neutron in a hydrogenous medium like water or paraffin is capture by a proton to form a deuteron; but, since the cross section for this reaction is quite small compared with the cross section for scattering, a neutron after reaching thermal energies makes about 150 further collisions before being captured. Paraffin and water are good substances to use for the slowing down of neutrons because the capture cross sections of oxygen and carbon are even much smaller than the hydrogen capture cross section. Heavy water is better than ordinary water because of the low probability of neutron capture by deuterium. Carbon (graphite) is also useful as a slowing-down medium; many more (about 120) collisions are necessary to reduce neutrons to thermal energies in carbon than in hydrogen, but after reaching thermal energies the neutrons can exist longer in carbon. In either substance the lifetime of a neutron before capture is only a fraction of a second.

Even if neutrons could be kept in a medium in which they would not eventually be captured, they would not exist very long. The systematics of β radioactivity predict that free neutrons are unstable and should decay

⁹The probabilities of the various values of n are given by the Poisson distribution, which is discussed in chapter 9, section D.

rather quickly into protons and electrons. This decay was observed in 1950 by A. H. Snell and by J. M. Robson with reactor neutrons that were in free flight in vacuum. The energy released in the disintegration is 0.78 MeV, and the half life is 10.6 min.

Thermal Distribution. It should be apparent that not all thermal neutrons have the same energy. After neutrons are slowed to energies comparable to thermal agitation energies they may either lose or gain energy in collisions, and the result is a Maxwellian distribution of velocities in which the fraction of the total number of neutrons with velocity between v and $v + dv$ is given by

$$F(v) dv = 4\pi^{-1/2} \left(\frac{M}{2kT}\right)^{3/2} v^2 e^{-Mv^2/2kT} dv. \quad (6-41)$$

Here M is the neutron mass, T is the absolute temperature, and k is the Boltzmann constant. Some properties of this distribution, usually derived in books on the kinetic theory of gases, are that the **most probable velocity** is

$$v_m = \left(\frac{2kT}{M}\right)^{1/2},$$

the **average velocity** is

$$\bar{v} = \left(\frac{8kT}{\pi M}\right)^{1/2} = \frac{2v_m}{\pi^{1/2}},$$

and the average kinetic energy is $\bar{E} = \frac{3}{2}kT$. The average energy of the neutrons depends on the temperature of the slowing-down medium. At very low temperatures the Maxwellian distribution function becomes a poor approximation because of the discrete energy levels of the bound atoms of the medium. At all temperatures the approximation can be poor if the neutron path in the medium is too short or if the distribution is seriously altered by neutron absorption or leakage from the surface.

A significant point is the distinction between the velocity distribution present in a medium and that felt by a sample placed in the medium. The two distributions are different because the probability that a particular neutron will strike the sample in a given time is proportional to v . It is the altered or weighted distribution, denoted here by $F'(v) dv$, that is significant in any transmutation or cross section computation:

$$F'(v) dv = 2\left(\frac{M}{2kT}\right)^2 v^3 e^{-Mv^2/2kT} dv. \quad (6-42)$$

E. RADIATION PROTECTION

The biological effects of radiation are brought about through chemical changes in the cells caused by ionizations, excitations, dissociations, and

atom displacements. In determining radiation effects on living organisms, whether from external radiation or from ingested or inhaled radioactive material, we must take into consideration not only the total dosages of ionization produced in the organism but also such factors as the density of the ionization, the dosage rate, the localization of the effect, and the rates of administration and elimination of radioactive material.

Apart from various medical procedures there is no evidence that the net direct effect of radiation on man is anything but harmful. In the absence of other clinical indications it is probable that even some diagnostic procedures that entail radiation have a greater chance of inducing rather than revealing a morbid condition. Thus except for the unavoidable background radiation, exposure to radiation is acceptable only on the basis of a risk/benefit analysis. It is, unfortunately, not yet possible to measure in a persuasive fashion the risk involved through exposure to small quantities of radiation. It is this fact that is at the root of much of the controversy on this subject.

Dosimetry in Radiation Protection (M1, M2). The unit of radiation dosage that is used in radiation protection is the **roentgen equivalent man (rem)**. The dosage in rems is equal to that in rads (defined on p. 7) multiplied by the relative damage caused by various kinds of radiation. The latter quantity depends on several factors, the most important of which is the density of ionization that in biological studies is often measured by the **linear energy transfer (LET)**, the energy that is deposited per unit path length. Note that the physical principles of LET have been outlined in the discussion of stopping power (dE/dx). Thus the dose equivalent in rems is given by the dose in rads multiplied by the **quality factor (QF)**.¹⁰ Approximate values of QF are given in table 6-2. The ranges of values in that table reflect the energy dependence of LET and thus of QF; it is prudent to use the upper limit in the absence of persuasive evidence to the contrary.

As an example of the practical application of some of the concepts discussed, we estimate the dosage rate in rads per hour to be expected at a distance of 50 cm from a 100-mCi ^{60}Co source. Each disintegration of ^{60}Co is accompanied by two γ quanta with energies 1.17 and 1.33 MeV; for simplicity we use for each an average energy of 1.25 MeV. The source emits $2 \times 100 \times 3.7 \times 10^7 = 7.4 \times 10^9$ quanta per second. At a distance of 50 cm the γ flux is $7.4 \times 10^9 / (4\pi \times 2500) = 2.3 \times 10^5$ photons $\text{cm}^{-2} \text{s}^{-1}$ or $2.3 \times 10^5 \times 1.25 \times 10^6 = 2.9 \times 10^{11} \text{ eV cm}^{-2} \text{s}^{-1}$. Since at an energy of 1.25 MeV the mass absorption

¹⁰ In the older literature the relative damage caused by various kinds of radiation was measured by the **relative biological effectiveness (RBE)**. This quantity is now reserved for more precise studies in radiobiology and is not used in the transformation from dose to dose equivalent in radiation protection. In the SI system the unit of radiation dose equivalent is the **sievert**, which is defined as the dose in gray (Gy) multiplied by the QF. See chapter 1, p. 7, for the definition of the gray.

where λ_c is in angstroms, R is the orbit radius in meters, E the electron energy in GeV, and B the magnetic field in tesla. Toward the short-wavelength side of λ_c the intensity drops rapidly, whereas it rises slightly to a peak at about $4\lambda_c$ and then decreases slowly toward still longer wavelengths (figure 15-14). In present-day synchrotrons (energies of a few billion electron volts, orbit radii of the order of 10 m) λ_c values are in the range of 1–10 Å (corresponding to photon energies of between 12 and 1 keV); synchrotron radiation is thus of no particular interest for nuclear research. However, it has become a very important tool in other fields including solid-state physics, radiation chemistry, photoelectron spectroscopy, and X-ray crystallography (W2). Electron storage rings for energies up to several billion electron volts and designed to serve as dedicated sources of synchrotron radiation are being built in several laboratories. Intensities of the order of 10^{13} photons $s^{-1} \text{Å}^{-1} \text{mrad}^{-1}$ per milliampere of circulating current can be achieved, and some of the designs call for circulating beams up to 1 A. Photons in otherwise unattainable energy and intensity ranges thus become available.¹¹ Furthermore, the fact that photons are emitted tangentially all around the azimuth of a machine makes it possible to perform many experiments simultaneously.

C. NEUTRON SOURCES

Radioactive Sources. Neutrons are produced in nuclear reactions and decay. Several naturally occurring and several artificially produced α and γ emitters can be combined with a suitable light element to make useful neutron sources (O1). Because of the short ranges of the α particles, α emitters must be intimately mixed with the light element (usually beryllium because it gives the highest yield). Such sources necessarily give neutrons with energies spread over a wide range. A γ emitter may be enclosed in a capsule surrounded by a beryllium or deuterium oxide target. (Only beryllium and deuterium have (γ, n) thresholds below 5 MeV.) Some of these sources can, in principle, give monoenergetic neutrons. However, because of neutron and γ -ray scattering in targets of practical thickness, the actual spectrum usually has an energy spread of about 30 percent, and the average energy is roughly 20 percent below the expected maximum value. Some useful sources are listed in table 15-1.

Since spontaneous fission, like any fission process, is always accompanied by neutron emission, a sample of a nuclide that undergoes spontaneous fission can serve as a neutron source. At present by far the most

¹¹ Further enhancement of intensities in particular wavelength regions is possible by means of so-called wigglers, which produce local regions of smaller radius of curvature. Particularly interesting are helical wigglers (K1); they produce photon spectra that are much more sharply peaked than those shown in figure 15-14.

Table 15-1 Alpha- and Gamma-Ray Neutron Sources

Source	Main Reaction	<i>Q</i> (MeV)	Neutron Energy (MeV)	Neutron Yield (per 10^6 dis)
Ra + Be(mixed)	${}^9\text{Be}(\alpha, n){}^{12}\text{C}$	5.65	up to 13	460
Po + Be (mixed)	${}^9\text{Be}(\alpha, n){}^{12}\text{C}$	5.65	up to 11, av. 4	80
Ra + B (mixed)	${}^{11}\text{B}(\alpha, n){}^{14}\text{N}$	0.28	up to 6	180
${}^{239}\text{Pu} + \text{Be}$ (mixed)	${}^9\text{Be}(\alpha, n){}^{12}\text{C}$	5.65	up to 11	60
Ra + Be (separated)	${}^9\text{Be}(\gamma, n){}^8\text{Be}^a$	-1.67	<0.6	0.9 ^b
Ra + D ₂ O (separated)	${}^2\text{H}(\gamma, n){}^1\text{H}$	-2.23	0.1	0.03 ^b
${}^{24}\text{Na} + \text{Be}$	${}^9\text{Be}(\gamma, n){}^8\text{Be}^a$	-1.67	0.8	3.8 ^b
${}^{24}\text{Na} + \text{D}_2\text{O}$	${}^2\text{H}(\gamma, n){}^1\text{H}$	-2.23	0.2	7.8 ^b
${}^{88}\text{Y} + \text{Be}$	${}^9\text{Be}(\gamma, n){}^8\text{Be}^a$	-1.67	0.16	2.7 ^b
${}^{88}\text{Y} + \text{D}_2\text{O}$	${}^2\text{H}(\gamma, n){}^1\text{H}$	-2.23	0.3	0.08 ^b
${}^{124}\text{Sb} + \text{Be}$	${}^9\text{Be}(\gamma, n){}^8\text{Be}^a$	-1.67	0.02	5.1 ^b
${}^{140}\text{La} + \text{Be}$	${}^9\text{Be}(\gamma, n){}^8\text{Be}^a$	-1.67	0.6	0.06 ^b
${}^{140}\text{La} + \text{D}_2\text{O}$	${}^2\text{H}(\gamma, n){}^1\text{H}$	-2.23	0.15	0.2 ^b

^aThe product ${}^8\text{Be}$ is unstable and decomposes in less than 10^{-14} s into two ${}^4\text{He}$ nuclei.

^bThe photoneutron yields are given for 1 g of target (D_2O or Be) at 1 cm from the γ -ray source.

practical nuclide for this purpose is ${}^{252}\text{Cf}$, which has a half life of 2.64 y, decays 96.9 percent by α emission, 3.1 percent by spontaneous fission, and emits on the average 3.76 neutrons per fission. Thus ${}^{252}\text{Cf}$ sources emit about 2.3×10^9 neutrons $\text{mg}^{-1} \text{s}^{-1}$, along with approximately ten times that many α particles.

Neutron-Producing Reactions with Accelerators. Much more copious sources of neutrons than can be obtained with radioactive α and γ emitters are available with ion accelerators. The reaction ${}^2\text{H}(d, n){}^3\text{He}$ (often called a *d-d* reaction) is exoergic ($Q = +3.27$ MeV), and, because the potential barrier is low, good neutron yields can be obtained with deuteron energies as low as 100–200 keV. With thick targets of solid D_2O , the yields are about 0.7, 3, and 80 neutrons per 10^7 deuterons at 100 keV, 200 keV, and 1 MeV deuteron energy, respectively. Direct-voltage accelerators are often used to produce the *d-d* reaction. The neutrons are monoenergetic if monoenergetic deuterons of moderate energies (up to a few million electron volts) fall on a sufficiently thin target.

Even more widely used is the *d-t* reaction: ${}^3\text{H}(d, n){}^4\text{He}$. Tritium ($t_{1/2} = 12.33$ y) has become available in large quantities. For use as a target it is usually adsorbed on zirconium or titanium. Neutron yields of about 150 per 10^7 deuterons are obtained at 200 keV. The reaction has a strong resonance at 100 keV deuteron energy and can be a remarkable source of neutrons from

very-low-energy deuterons. The reaction is exoergic with $Q = 17.6 \text{ MeV}$, and monoenergetic neutrons of about 14 MeV are produced from a thin target.

For a controlled source of monoenergetic neutrons of very low energy (down to about 30 keV) the $^7\text{Li}(p, n)^7\text{Be}$ reaction is suitable, especially when produced with the protons of well-defined energy available from electrostatic generators. The reaction is endoergic ($Q = -1.644 \text{ MeV}$) and has a threshold of 1.88 MeV . Advantage may be taken of the differences in neutron energy in the forward and backward (and intermediate) directions.

With X rays from electron accelerators neutrons can be produced by means of the $^9\text{Be}(\gamma, n)$ or $^2\text{H}(\gamma, n)$ reactions. The yields of these reactions go up quite sharply with energy. With an electrostatic generator operating at 2.5 MeV with $100 \mu\text{A}$ electron current the neutron yield per gram of beryllium is $7 \times 10^7 \text{ s}^{-1}$; at 3.2 MeV the corresponding figure is $4 \times 10^8 \text{ s}^{-1}$.

When deuteron and proton beams above a few million electron volts are available a number of reactions can be used to produce copious quantities of neutrons. The $^2\text{H}(d, n)^3\text{He}$ reaction discussed previously and the $^9\text{Be}(d, n)^{10}\text{B}$ reaction are especially favorable for neutron production. The latter reaction has a positive Q value of 3.80 MeV , but the neutrons are far from monoenergetic; deuterons of $E \text{ MeV}$ produce a distribution of neutron energies up to about $E + 3.5 \text{ MeV}$. The neutron yield goes up rapidly with deuteron energy, from $10^8 \text{ s}^{-1}(\mu\text{A})^{-1}$ at 1 MeV to $10^{10} \text{ s}^{-1}(\mu\text{A})^{-1}$ at 8 MeV and $3 \times 10^{10} \text{ s}^{-1}(\mu\text{A})^{-1}$ at 14 MeV . With both reactions mentioned the neutrons are emitted largely in the forward direction and both reactions have been used extensively for neutron therapy and neutron radiobiology.

Considerably higher neutron energies than with beryllium targets are obtained by deuteron bombardment of lithium targets, since the reaction $^7\text{Li}(d, n)^8\text{Be}$ is exoergic by 15 MeV .¹² The neutron yield is only about one third that of the $^9\text{Be}(d, n)^{10}\text{B}$ reaction. Neutrons are also obtained in the bombardment of almost any element with fast protons, deuterons, or α particles. The yields and energies vary from reaction to reaction, but if a neutron bombardment is needed for the activation of some substance it is often sufficient to place the sample near a cyclotron target that is being bombarded by deuterons, even if the target is not beryllium or lithium.

In the bombardment of targets with deuterons of much higher energy ($>100 \text{ MeV}$), high-energy neutrons are emitted in a rather narrow cone in the forward direction as a result of deuteron stripping (see p. 147). The energy distribution of these neutrons is approximately Gaussian, with the maximum at half the deuteron energy.

When high-energy protons strike target nuclei they produce neutrons in

¹² This reaction is to be used for the production of very intense fast-neutron beams for testing fusion reactor materials; a high-current deuteron linac for this purpose will be operating at Hanford, Washington, in the 1980s.